NUMERICAL AND EXPERIMENTAL INVESTIGATIONS ON NONSTATIONARY VIBRATIONS OF NONLINEAR SYSTEMS

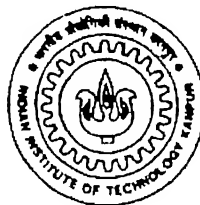A Thesis Submitted
in Partial Fulfillment of the Requirements
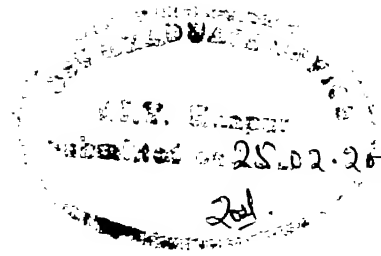for the Degree of

MASTER OF TECHNOLOGY

February, 2000

by

AMOD CHANDRASHEKHAR GHANGURDE

DEPARTMENT OF MECHANICAL ENGINEERING
INDIAN INSTITUTE OF TECHNOLOGY
KANPUR – 208016 (INDIA)

CERTIFICATE

It is certified that the work contained in the thesis entitled, "**NUMERICAL AND EXPERIMENTAL INVESTIGATIONS ON NONSTATIONARY VIBRATIONS OF NONLINEAR SYSTEMS**" by *Mr. Ghangurde Amod Chandrashekhar* has been carried out under my supervision and that this work has not been submitted elsewhere for a degree.

Nalinaksh Vyas.

Dr. N.S.Vyas

(Professor)

Department of Mechanical Engineering,

February, 2000

Indian Institute of Technology, Kanpur.

ACKOWLEDGEMENTS

CONTENTS

LIST OF FIGURES

ABSTRACT

Nonstationary vibratory phenomenon is exhibited by machines and components, when they are subjected to variable frequency operations like start-up and shut-down. While nonstationary behaviour of linear systems are fairly well documented, information on nonlinear systems is scant due to lack of analytical procedures. The present study attempts to carry out numerical and experimental exercises to understand such behaviour. The exercise is restricted to systems involving spring nonlinearities only. Damping is taken to be linear in the entire analysis. Four different types of spring nolinearities are studied – (i) polynomial nonlinearity; (ii) symmetric square nonlinearity (iii) bearing nonlinearity (iv) bilinear nonlinearity. Single degree freedom systems are considered and their response is numerically obtained through fourth order Runge-Kutta technique, employing MATLAB Simulink Toolbox. The results in the first case are compared to those obtained using the approximate asymptotic analysis. In the remaining cases system response is sought to be understood through equivalent piecewise polynomial form expressions. Experimental investigations are carried out through Virtual Instrumentation techniques for signal generation and data acquisition. The response of a cantilever beam, subjected to frequency swept excitation is reported.

CHAPTER 1

INTRODUCTION

In most vibration analysis problems an acceptable idealization and simplification is made - that the system components are time independent and linear. Thus masses, restoring forces, frequencies and amplitudes of external excitation are considered to be time independent. Oscillatory motion of such a system is called stationary. When one or more of the system or external excitation components vary with time, the system is said to be non-stationary and the oscillatory motion of such a system is non-stationary. Nonstationary vibratory phenomenon is exhibited by machines and components, when they are subjected to variable frequency operations. Start-up and shut-down operations of machinery are common instances of occurrences of such phenomenon. Many reciprocating engines, turbines are operated above their critical speed and pass through this critical speed during start-up and shut-down processes. The dynamic stresses experienced during such processes and their duration need to be analysed for safe operations. The objective of the present study is to analyse nonstationary vibrations of nonlinear systems under variable frequency excitation. While procedures for analysis of linear systems subjected to excitation forces, with frequency varying with time, are fairly well established, very few studies are available on the behaviour of nonlinear systems under such excitation conditions. For linear systems, it is known that the maximum amplitude during a frequency sweep will be smaller than if the excitation frequency was held constant, and further, that an apparent shift in the position of critical will occur. The lack of information of such nonstationary phenomenon of nonlinear systems, is primarily due to the considerable mathematical complexity of such problems and a complete absence of closed form analytical solutions.

The problem of non-stationary oscillations in mechanical and electrical systems was discussed by Lewis (1932). He presented an exact solution of the problem of running a

system having a single degree of freedom and linear damping through its critical speed from rest at a uniform acceleration rate. The analytical solutions of non-stationary vibrations were first proposed by Krylov and Bogolyubov (1961), through their method of asymptotic expansions. They gave an effective method of investigation, applicable to an extensive class of oscillatory processes described by nonlinear equations with varying coefficients. Reference can be made to studies by Gasch et al (1979), Vyas et al (1986), Irretier (1984), Nonami et al (1988) for analysis of problems concerning rotating shaft and blading systems during acceleration through critical speeds. While the stationary response of nonlinear systems is characterised (as distinct from stationary response of linear systems) by presence of subharmonic frequencies and an inclined backbone curve, information on the response during nonstationary conditions is scant. An asymptotic approximation of the envelope of the response of a Duffing oscillator under linearly varying excitation frequency, based on slowly varying parameters was developed by Mitropol'skii (1965). Agrawal and Ewan-Iwanowski (1976) investigated non-stationary response for various kinds of summed-and-differential harmonic oscillations. They obtained approximate solutions by means of the asymptotic method and gave amplitude variation curves calculated numerically. In experiments were also carried out for verification of analytical results. Recently, Ishida et al (1992) studied non-stationary oscillations of rotating shaft with nonlinear spring characteristics during acceleration through a major critical speed. Approximate solutions for steady state and non-stationary oscillations by asymptotic method and proposed a complex FFT method. The method is based on the signal processing concept. Spectral distribution is obtained for the entire time history of accelerated or decelerated signal. A desired frequency component is extracted by filtering. This extracted frequency component is transformed into time history by inverse FFT algorithm. The amplitude variation of this transformed signal is then plotted.

A major limitation of the studies on nonlinear systems is that procedures of analysis exist only for a very limited class of nonlinear functions. Moreover the solutions are approximate and apply with reasonable accuracy only within certain range of operations. If the amount of non-linearity is not too large, analytical methods may be used to yield an

approximate solution. If the amount of non-linearity is larger, analytical methods may not be sufficient and solution may be possible only by numerical or graphical methods. Thus, any solution applies for only one particular set of conditions. Furthermore, the process of obtaining solution is usually tedious, requires considerable manipulation if good accuracy is to be obtained. The focus of the present study is to study the nonstationary response behavior of linear and nonlinear single degree of freedom systems, through numerical simulation. Tools available in MATLAB software have been employed for numerical simulation. Various kinds of commonly occurring nonlinearities in mechanical systems have been investigated. The analysis is carried out in terms of non-dimensional parameters, to the extent possible. The response of linear systems subjected to variable frequency excitation is presented in Chapter 2. Response of four different types of nonlinear systems is investigated in Chapter 3. The results are analysed as functions of nonlinear parameters, damping and excitation frequency acceleration rates. Experimental work carried out on a laboratory set-up is described in Chapter 4. Conclusions and scope for further work are given in Chapter 5.

CHAPTER 2

NON-STATIONARY VIBRATIONS OF LINEAR SYSTEMS

Response of a linear single-degree of freedom system under frequency swept excitation is presented in this Chapter. This analysis is readily available in literature and is presented here, for the sake of completeness and later comparison with the response of nonlinear systems.

2.1 Equation of motion

For a simple mass, spring, dashpot system, Figure (2.1), acted upon by a sinusoidal force, with initial frequency ω_0 and changing at a constant rate α, the equation of motion can be written as

$$m\ddot{x} + c\dot{x} + kx = f_0 \sin(\omega_0 t + \frac{1}{2}\alpha t^2) \tag{2.1}$$

where a dot denotes differentiation with respect to time t, k and c are constants of proportionality for restoring force and damping respectively. m is the mass of the system.

Defining the following non-dimensional parameters

$$\tau = pt, \qquad r_0 = \omega_0/p, \qquad r_\alpha = \alpha/p^2,$$

$$\bar{x} = x/x_{st}, \qquad 2\zeta = c/k \qquad p = \sqrt{k/m}$$

with $x_{st} = f_0/k$

equation (2.1) is rendered in the following non-dimensional form:

$$\bar{x}'' + 2\zeta\bar{x}' + \bar{x} = \sin(r_0\tau + \frac{1}{2}r_\alpha\tau^2) \tag{2.2}$$

$$f_0 \sin(\omega_0 t + \frac{1}{2}\alpha t^2)$$
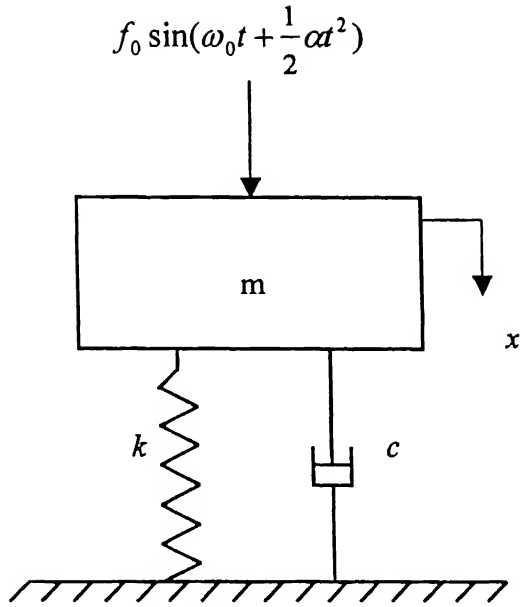
Fig. 2.1   Single degree of freedom non-stationary system
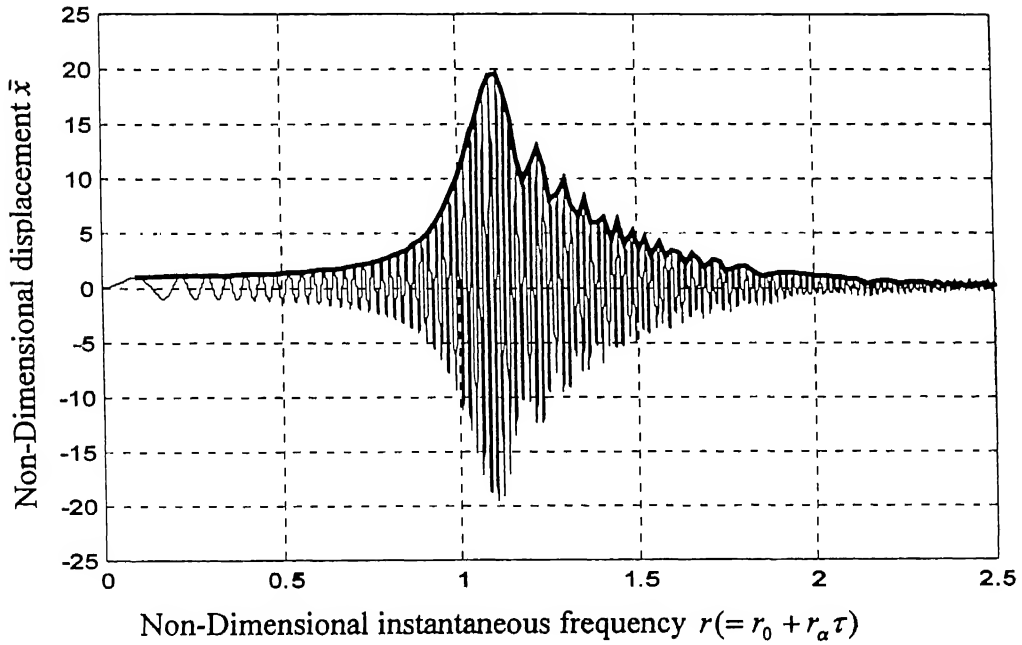
Fig. 2.2   Non-stationary response of linear system with amplitude envelop

5

2.2   Response Simulation

The response of the nondimensional governing equation (2.2) is simulated using MATLAB (Simulink toolbox). A sample program for the simulation of equation (2.2) on MATLAB is shown in Appendix 1. The numerical simulation is based on fourth-order Runge-Kutta technique.

Fig. 2.2 shows a typical numerically simulated response of equation (2.2), for a damping ratio, $\zeta = 0.01$ and rate of acceleration $r_a = 0.001$. The sweep is carried out from initial frequency, $r_0 = 0$ to a final nondimensional frequency value equal to 2.5. The response is shown by solid line and the dark solid line shows the envelope of the response, which defines the maximum amplitude attainable, during the process. Henceforth, in the present study, response is displayed only through the envelope curves, for better understanding of qualitative behavior of the system.

The response is studied as a function of different rates of acceleration and damping ratios. Fig. 2.3 describes the response envelope for three frequency sweep rates $r_a = 0.001$, 0.003 and 0.005. The damping ratio is kept constant ($\zeta = 0.01$). The stationary frequency response curve $r_a = 0$, is also shown in the figure. The resonant response amplitude, can be readily seen from the stationary response curve, to be equal to 50, which as expected is equal to the quality factor $1/2\zeta$. The resonant response frequency, on the nondimensional instantaneous frequency ($r = r_0 + \alpha\tau$) axis can be seen to be equal to 1. For the nonstationary cases ($r_a \neq 0$), the response can be seen to attain an apparent resonance, with maximum amplitude less than the resonant amplitude of the stationary case. Also this apparent resonance occurs not at instantaneous excitation frequency value $r = 1$, but at an instant shifted to the right of $r = 1$. These apparent resonant amplitudes can be seen to decrease with increasing rates of acceleration. Also the shift away from the instant $r = 1$, becomes more pronounced with increase in the acceleration rate. This can be explained by the fact that while the phenomenon of resonance does occur when the excitation frequency is equal to the system's natural frequency (i.e. $r = 1$), resonant amplitudes also need time to build up.
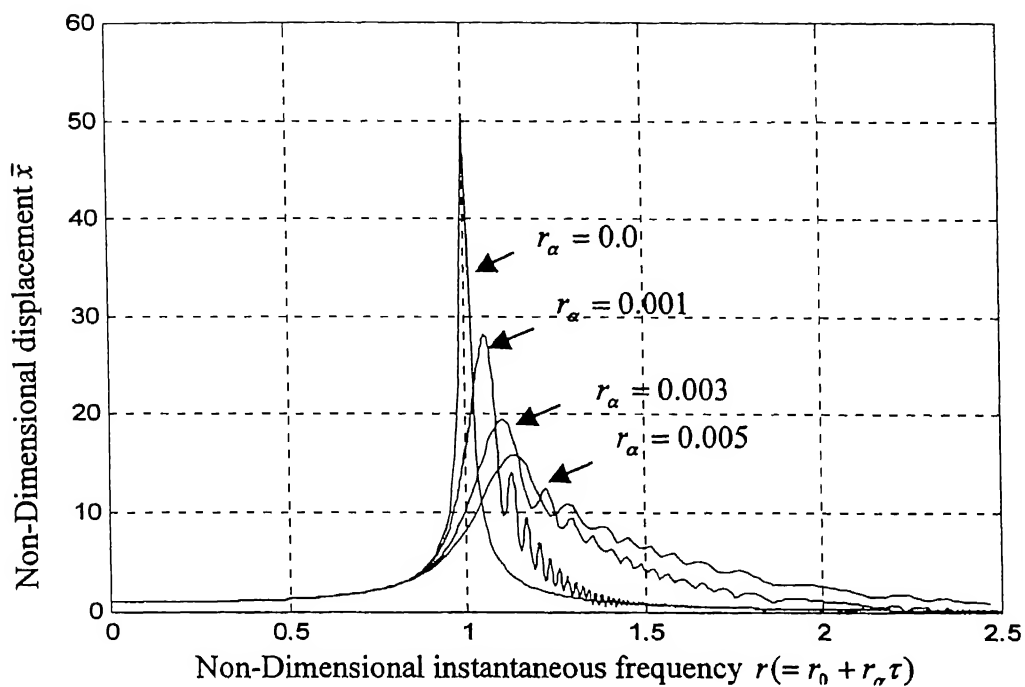
Fig. 2.3   **Influence of acceleration rate r_α (linear system)**
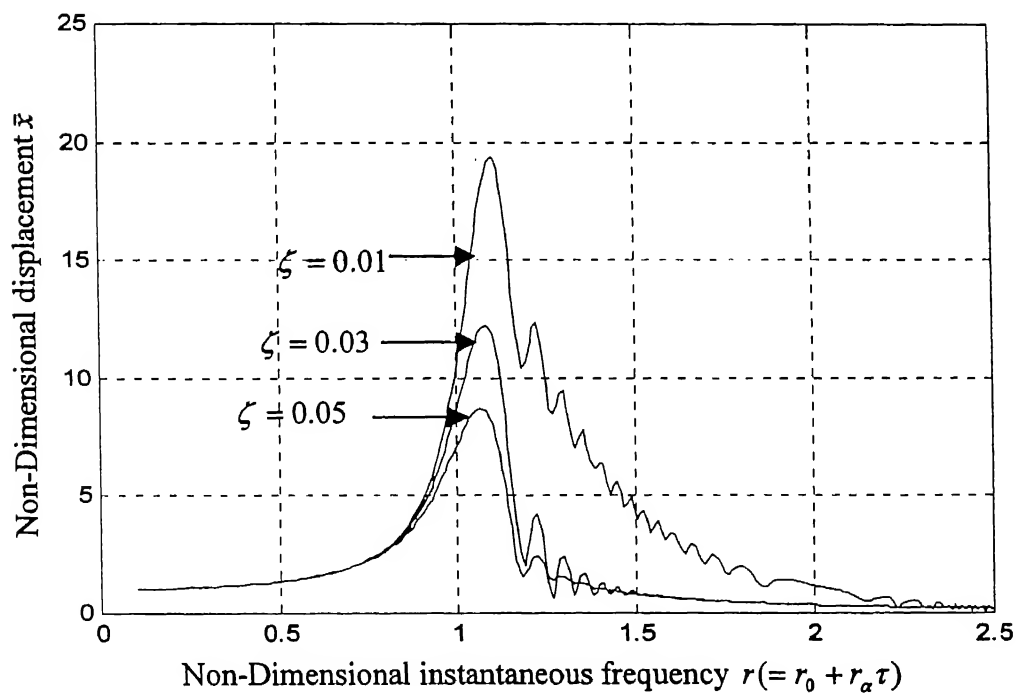
Fig. 2.4   **Influence of damping (linear system)**

7
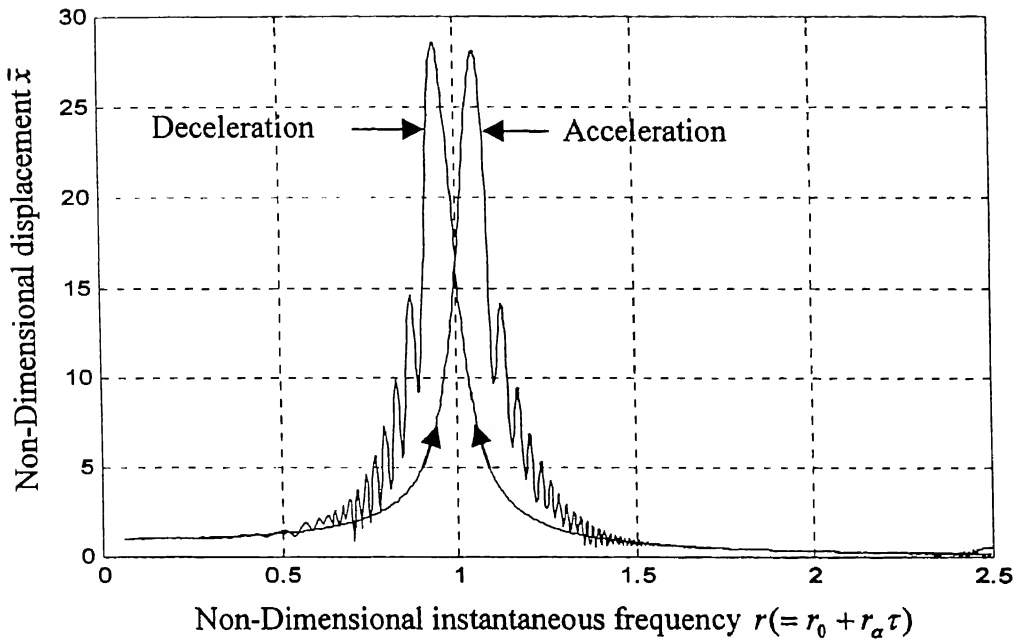
Fig 2.5   Acceleration and Deceleration for linear system

In the case of stationary vibrations at a constant excitation frequency, the system reaches its steady state value. However, sufficient time is not available to the system to reach steady state, when it is subjected to a frequency sweep. The amplitude of vibration does start increasing, when the instantaneous excitation frequency momentarily becomes equal to the natural frequency. In addition to the externally provided energy being utilised in building up resonant amplitudes, a portion of this energy is also utilised in accelerating the system. Under the influence of these two activities an apparent resonance is exhibited, with a vibratory amplitude, less than what would have been achieved, if the process were stationary, and at an instant shifted in the direction of frequency sweep. The higher is the acceleration rate, less is the time available to build resonant amplitudes, as seen in Figure 2.3. In absence, of a steady state, system can also be seen to exhibit the beat phenomenon, in the vicinity of the region $r = 1$. Fig. 2.4 shows the influence of the damping const ζ, and as expected higher values of damping effect greater suppression of

the resonant amplitude, without any other qualitative change in the behaviour. The behaviour under a negative frequency sweep rate, is shown along with an identical positive sweep rate in Fig. 2.5. The response pattern is practically symmetric about $r = 1$, with the maximum amplitude being attained at an instant shifted to the left of $r = 1$, which in the case of negative sweep rate is the direction of frequency change. The initial frequency in the case of negative sweep is 2.5, while the curve for positive sweep rate starts with a value of $r_0 = 0$. The minor difference in the peak response values is due to the difference in the initial conditions, in the two cases.

CHAPTER 3

NONSTATIONARY OSCILLATIONS OF NONLINEAR SYSTEMS

Nonlinearities in mechanical systems can arise from several sources. These are broadly classified into (i) geometrical nonlinearities – arising due to relatively large displacements and (ii) physical nonlinearities – arising due to nonlinear or multi-valued stress-strain relationships. This non-linearity may be present due to stiffening characteristics of material itself. For instance, an organic material such as rubber or leather used in couplings and vibration absorbers, have their modulus of elasticity increasing with elongation. Another example of variable flexibility is encountered in the case of cast iron or concrete structures. Elastic characteristics can be seen to vary with displacements in some steel springs as well. Natural frequencies of systems involving such elements depend on the amplitude of vibration. Another kind of nonlinearity is encountered in systems where the damping forces cannot be simply represented by linear functions of velocity. For instance, resistance of air or liquid, at considerable high speed, is taken to be proportional to the square of the velocity. The present study is restricted to systems involving spring nonlinearities only. Damping is taken to be linear in the entire analysis. Four different types of spring nolinearities are studied – (i) polynomial nonlinearity; (ii) symmetric square nonlinearity (iii) bearing nonlinearity (iv) bilinear nonlinearity. Single degree freedom systems are considered and their response is numerically obtained through fourth order Runge-Kutta technique, employing MATLAB Simulink Toolbox. The results in the first case are compared to those obtained using the approximate asymptotic analysis for the envelopes, as developed by Mitropol'skii (1965). In the remaining cases equivalent polynomial form expressions are obtained for the nonlinear functions for the interpretation of the numerical results. Results are obtained for both positive and negative sweep rates. The analysis is carried out in nondimensional form and the significant features of the nonstationary response associated with nonlinearity forms under consideration are presented.

3.1   Polynomial nonlinearity

A single degree of freedom system, with linear damping, excited by a sinusoidal force with a frequency constantly increasing with time, as given below is considered.

$$m\ddot{x} + c\dot{x} + f(x) = f_0 \sin(\omega_0 t + \frac{1}{2}\alpha t^2)$$ (3.1)

$f(x)$ is the non-linear restoring force, which is taken to be of the following general polynomial form.

$$f(x) = k_1 x + k_2 x^2 + k_3 x^3 + \ldots\ldots\ldots$$ (3.2)

Restricting to terms up to cubic, the following two cases are investigated

Case (1)   Cubic nonlinearity alone i.e. $k_1 \neq 0$, $k_2 = 0$, $k_3 \neq 0$.

Case (2)   Combined Square and Cubic nonlinearity i.e. $k_1 \neq 0$, $k_2 \neq 0$, $k_3 \neq 0$.

3.1.1   <u>Case (1)</u>   <u>Cubic nonlinearity alone</u> ($k_1 \neq 0$, $k_2 = 0$, $k_3 \neq 0$)

A system with cubic nonlinearity is the commonly known Duffing oscillator and is considered to be a benchmark system in nonlinear analysis. The governing equation (3.1) becomes

$$m\ddot{x} + c\dot{x} + k_1 x + k_3 x^3 = f_0 \sin(\omega_0 t + \frac{1}{2}\alpha t^2)$$ (3.3)

Response is numerically computed for both hard $(\beta > 0)$ and soft $(\beta < 0)$ springs. Defining the following parameters

$$\tau = pt, \qquad\qquad r_0 = \omega_0/p, \qquad\qquad r_\alpha = \alpha/p^2$$

$$\bar{x} = x/x_{st}, \qquad\qquad \bar{x}' = x'/x_{st}, \qquad\qquad \bar{x}'' = x''/x_{st} \qquad (3.3a)$$

$$\lambda = k_3 f_0^2/k_1^3, \qquad\qquad 2\zeta = c/mp \qquad\qquad p = \sqrt{k_1/m},$$

with $x_{st} = f_0/k_1$

equation (3.3) can be written in non-dimensional form as,

$$\bar{x}'' + 2\zeta\bar{x}' + \bar{x} + \lambda\bar{x}^3 = \sin(r_0\tau + \frac{1}{2}r_\alpha\tau^2)$$ (3.4)

In the above ζ is the linear damping ratio and λ is a nondimensional nonlinear parameter. It is to be noted here that λ, in addition to the nonlinear stiffness term k_3, involves the excitation force amplitude f_0 also. The response of equation (3.4) is numerically simulated in MATLAB. The Simulink model developed for the purpose is given in Appendix 2. The nondimensional response $\bar{x}$ is plotted in Fig. 3.1 (a) as a function of the instantaneous nondimensional excitation frequency $r\,(=r_0+r_\alpha\tau)$, for nonlinear parameter $\lambda=0.05$. The plot for the stationary response of the system is also shown dashed in this figure. This plot is obtained from the steady state response of the system for constant frequency excitation, as given by the following governing equation

$$\bar{x}'' + 2\zeta\bar{x}' + \bar{x} + \lambda\bar{x}^3 = \sin(r\tau) \tag{3.5}$$

(r is a constant, in the above)

The stationary response curve shows the features like the backbone curve and the jump phenomenon, characteristic to the Duffing oscillator. In contrast to a linear system the natural frequency of a Duffing oscillator is amplitude dependent and is characterised by the backbone curve. The backbone curve describing the relationship between the nondimensional nonlinear parameter λ, nondimensional excitation frequency r and the nondimensional amplitude A of vibration, can be written as (Stoker,1950).

$$\left[A(1-r^2)+3\lambda\frac{A^3}{4}\right]^2 + (2\zeta Ar)^2 = 1 \tag{3.6}$$

A two term Volterra series approximation of the response of equation (3.5), for small λ can be written as (Schetzen, 1979)

$$x(\tau) \approx \mathrm{Re}\{H_1(jr)e^{jr\tau}\} + \frac{3}{4}\mathrm{Re}\{H_3(jr,jr,-jr)e^{jr\tau}\} + \frac{1}{4}\mathrm{Re}\{H_3(jr,jr,jr)e^{j3r\tau}\}$$

$$= \mathrm{Re}\{H_1(jr)e^{jr\tau}\} + \frac{3}{4}\lambda\,\mathrm{Re}\{H_1^3(jr)H_1^*(jr)e^{jr\tau}\} + \frac{1}{4}\mathrm{Re}\{\lambda H_1^3(jr)H_1(3jr)e^{j3r\tau}$$

$$x(\tau) = |H_1(jr)|\cos[r\tau-\theta(r)] + 3\frac{\lambda}{4}|H_1(jr)|^4\cos[r\tau-2\theta(r)]$$

$$+ \frac{\lambda}{4}|H_1(jr)|^3|H_1(j3r)|\cos[3r\tau-3\theta(r)-\theta(3r)] \tag{3.7}$$

12
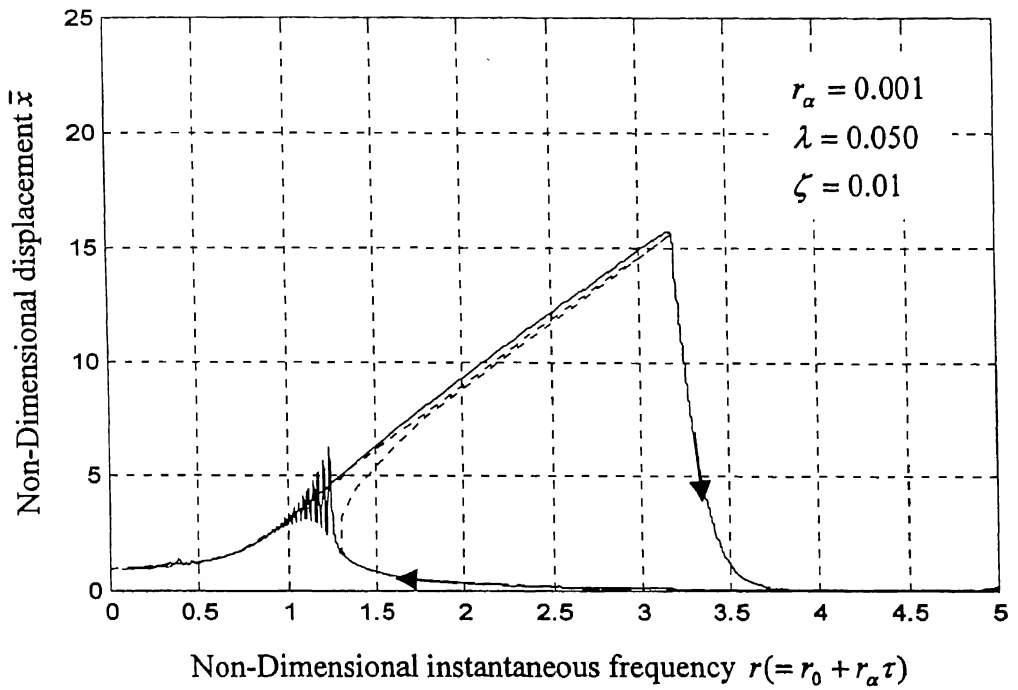
Fig. 3.1(a) **Steady and non-stationary response of cubic non-linear hard system ($\lambda > 0$)**
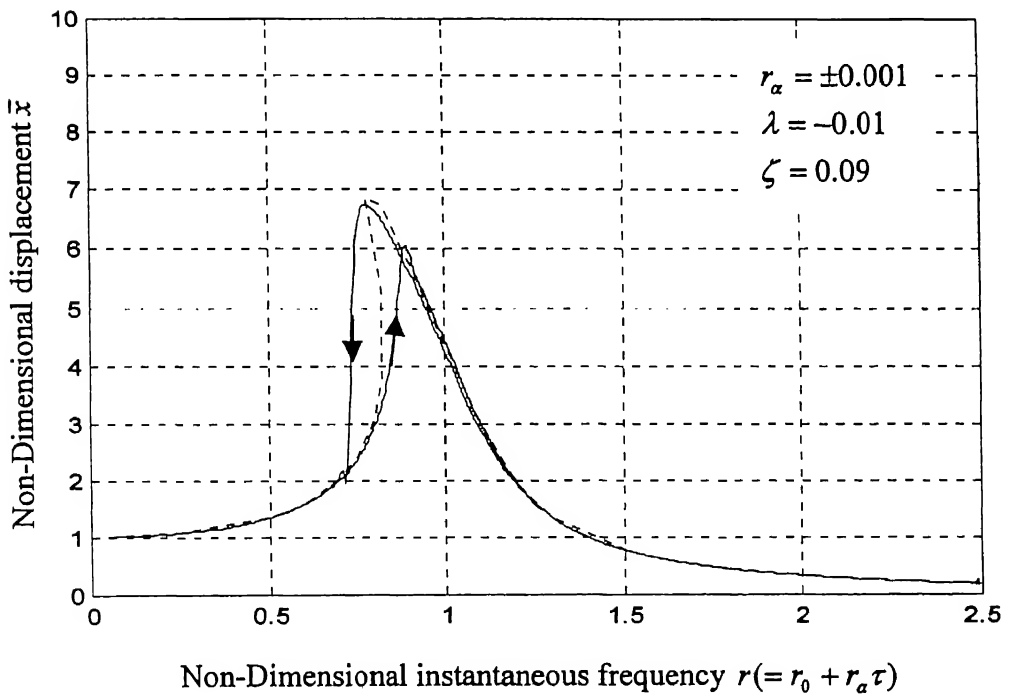
Fig. 3.1(b) **Steady and non-stationary response of cubic non-linear soft system($\lambda < 0$)**

Fig. 3.2(a) **Influence of cubic non-linear parameter λ during acceleration (hard spring, $\lambda > 0$)**
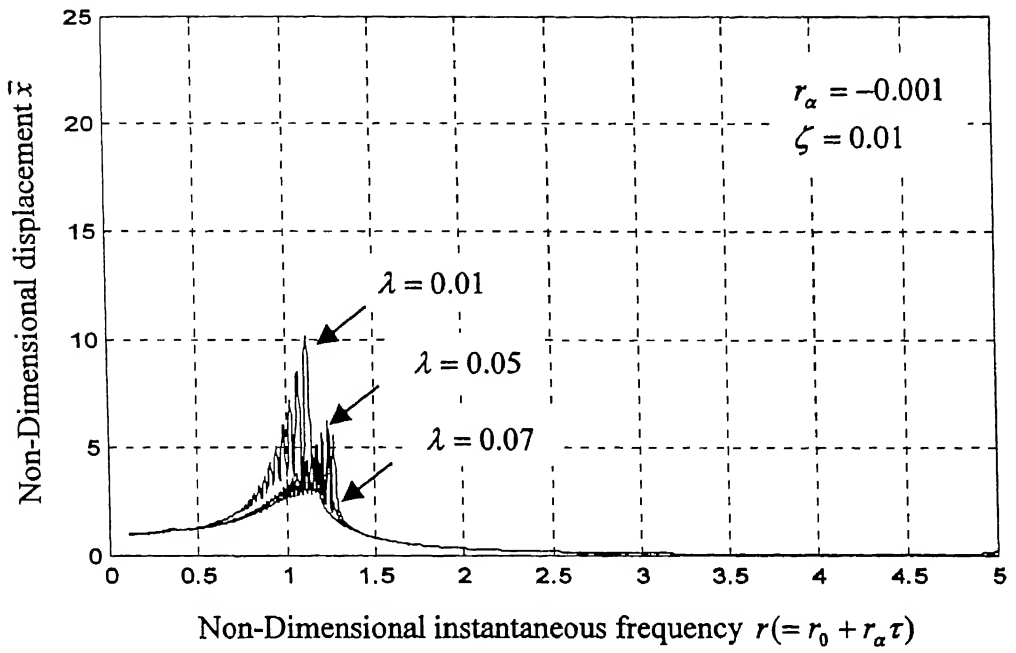
Fig 3.2(b) Influence of cubic non-linear parameter λ during deceleration (hard spring, $\lambda > 0$)

The figure shows a plot with axes labeled "Non-Dimensional displacement $\bar{x}$" (vertical, from 0 to 25) and "Non-Dimensional instantaneous frequency $r(= r_0 + r_\alpha \tau)$" (horizontal, from 0 to 5). Parameters shown: $r_\alpha = -0.001$, $\zeta = 0.01$. Three curves are labeled $\lambda = 0.01$, $\lambda = 0.05$, and $\lambda = 0.07$.

In the above expressions $H_1(jr)$ is the first order Frequency Response Function (FRF) of the equation and is given by

$$H_1(jr) = 1/[(1-r^2) + j(2\zeta r)] \tag{3.7a}$$

The response given by equation (3.7) comprises of harmonics at the excitation frequencies r and a subharmonic at frequency equal to $3r$. The amplitude of the first harmonic then can be written as

$$A_1 = |H_1(jr)|\left[1 + 3\frac{\lambda}{4}|H_1(jr)|^3 e^{-j\theta(r)}\right] \tag{3.8}$$

and that of the subharmonic as

$$A_3 = \frac{\lambda}{4}|H_1(jr)|^3|H_1(j3r)| \tag{3.9}$$

The subharmonic resonance can be seen in Fig.3.1(a).

The nonstationary response in Fig.3.1 (a) has been computed for both positive and negative rates of acceleration, r_α. The magnitude of r_α is 0.001. During positive acceleration, the initial frequency r_0, is taken as zero, while in the negative acceleration case the initial frequency, r_0 is equal to 5.0 and the frequency range is swept back to zero. The corresponding behaviour for a soft spring ($\lambda = -0.01$) is shown in Fig.3.1 (b). Fig. 3.2 (a) shows the influence of various values of the nonlinear parameter λ, for hard spring case (λ positive) with acceleration rate $r_\alpha = 0.001$, while Fig 3.2(b) shows the corresponding behaviour for a negative acceleration. Results for various negative values of λ are shown in Figs.3.3 (a), (b). The influence of different acceleration and deceleration rates for hard spring is depicted in Fig. 3.4. The influence of damping on the overall response is shown in Fig.3.5 with acceleration rate $r_\alpha = 0.001$. In Figs. 3.2 to 3.5, wherever possible, subharmonics are zoomed and presented.
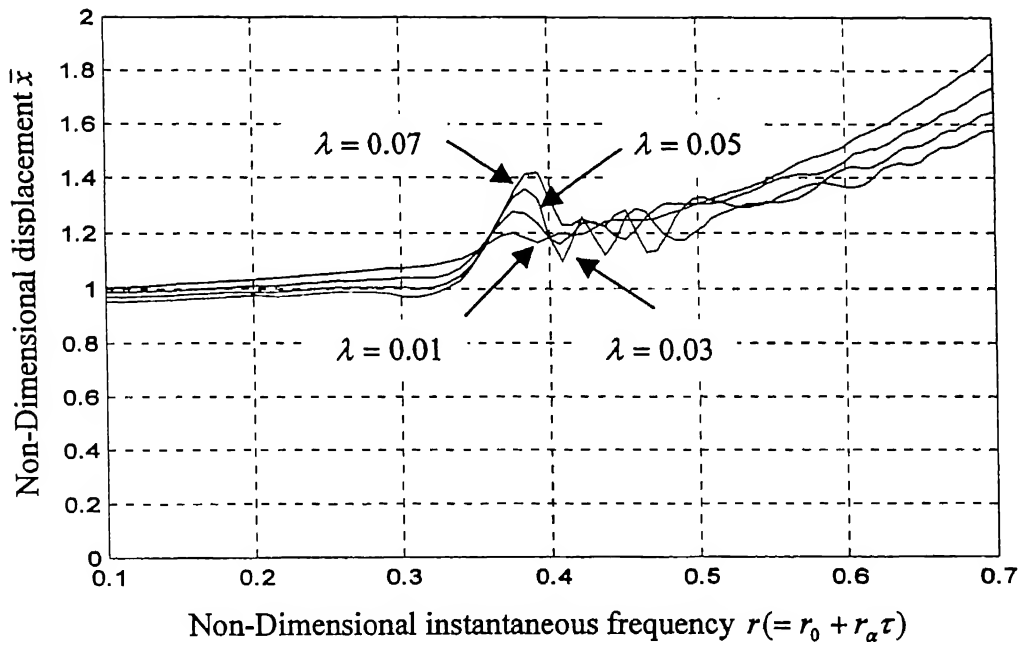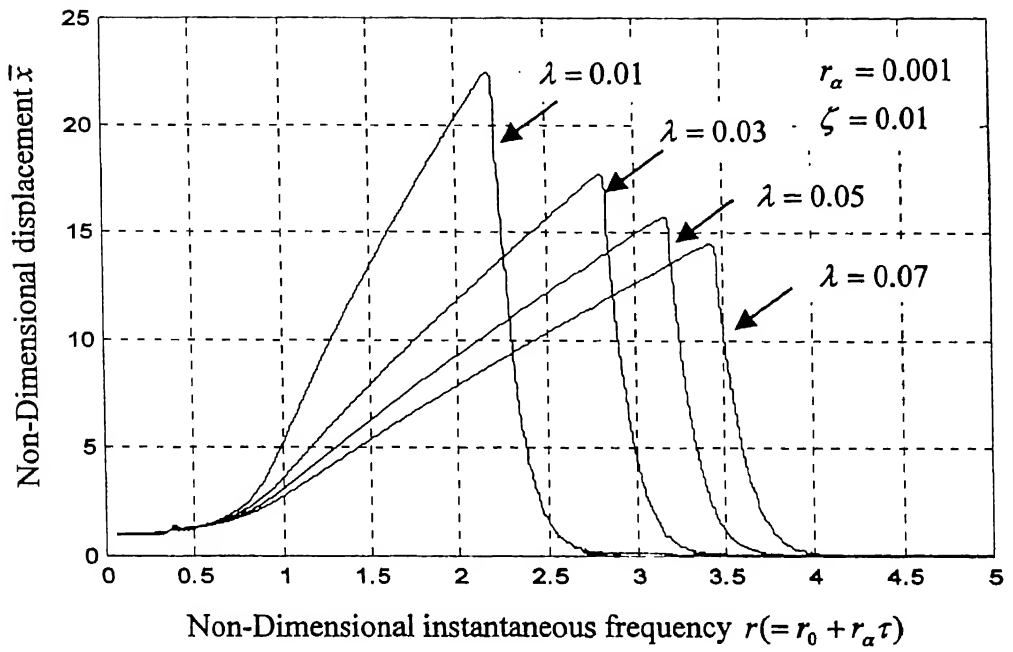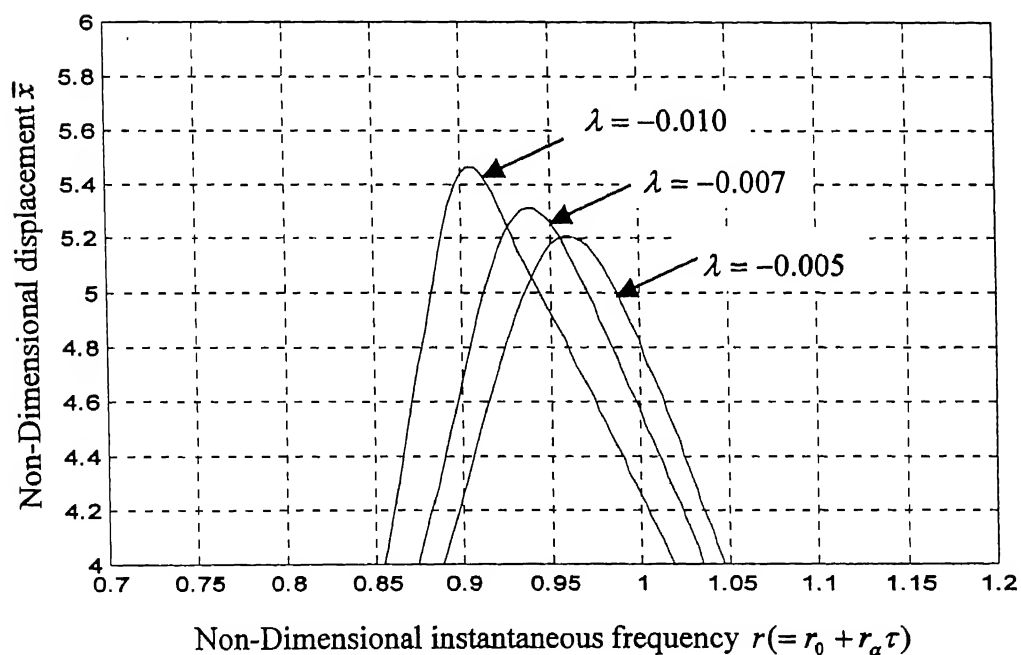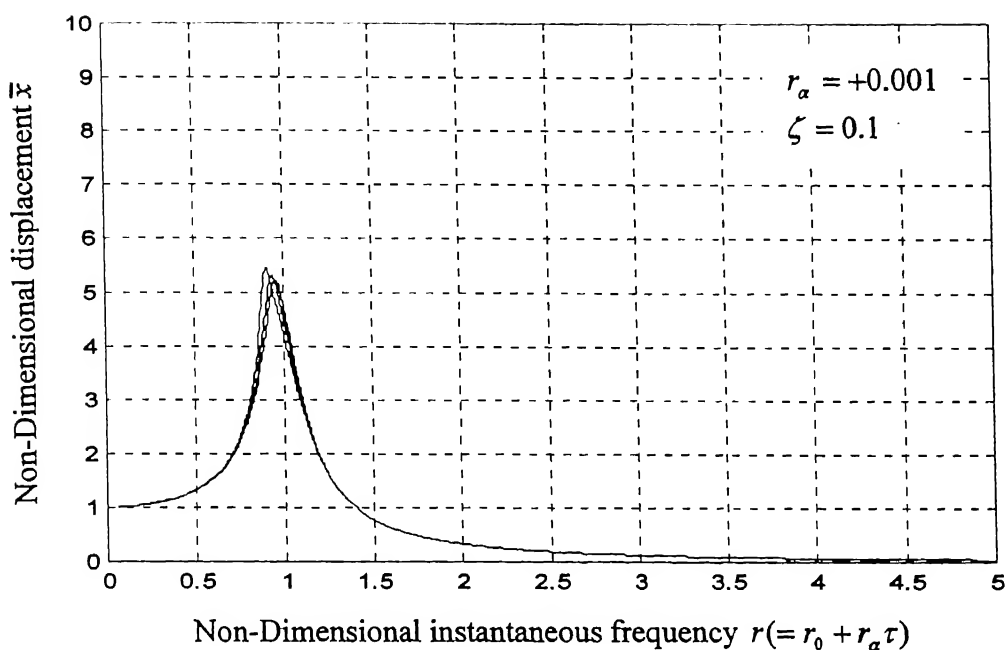
Fig. 3.3(a)   Influence of cubic non-linear parameter λ during acceleration

(soft spring, $\lambda < 0$)

17
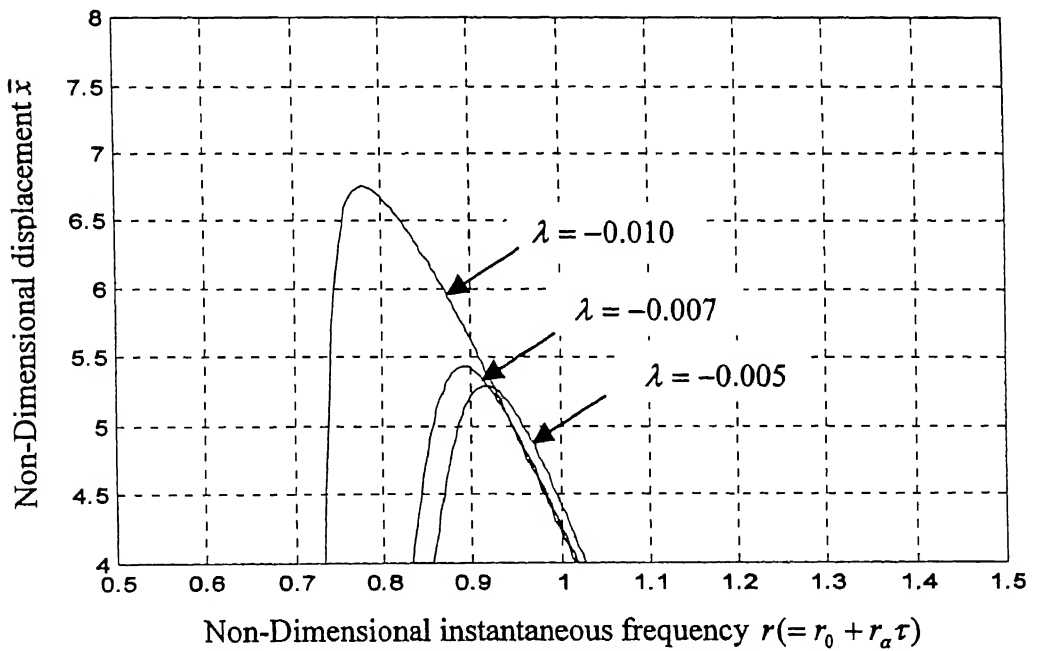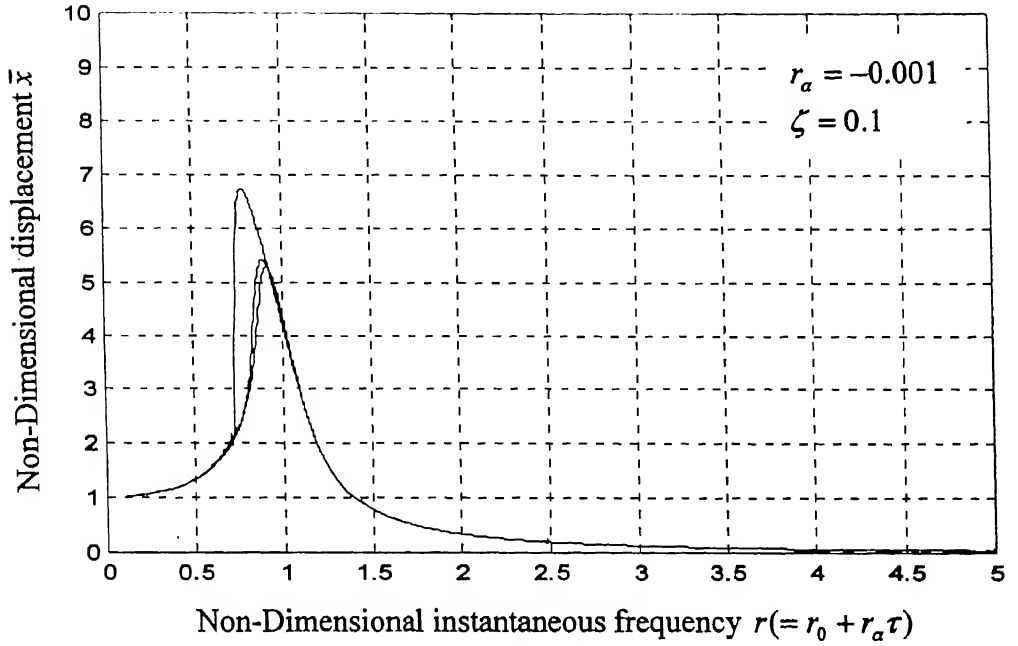
Fig. 3.3(b)   Influence of cubic non-linear parameter λ during deceleration (soft spring, $\lambda < 0$)

18

Top plot:
- Y-axis: Non-Dimensional displacement $\bar{x}$ (0 to 25)
- X-axis: Non-Dimensional instantaneous frequency $r(=r_0 + r_\alpha\tau)$ (0 to 5)
- $\lambda = 0.05$
- $\zeta = 0.01$
- $r_\alpha = 0.0003$
- $r = 0.001$
- $r_\alpha = 0.003$
- $r_\alpha = 0.005$

Bottom plot:
- Y-axis: Non-Dimensional displacement $\bar{x}$ (0.4 to 1.8)
- X-axis: Non-Dimensional instantaneous frequency $r(=r_0 + r_\alpha\tau)$ (0.2 to 0.6)
- $r_\alpha = 0.0003$
- $r_\alpha = 0.001$
- $r_\alpha = 0.003$
- $r_\alpha = 0.005$

Fig. 3.4   Influence of acceleration rates (hard spring, $\lambda > 0$)

19

Fig. 3.5 Influence of damping (hard spring, $\lambda > 0$)

The following conclusions can be drawn from Figs. 3.1 to 3.5 on the nonstationary vibrations of the Duffing oscillator -

(a) The maximum response achieved by the system decreases with increase in the acceleration rate. The sharpness of the resonance curve also becomes less pronounced as the transition through resonance becomes faster. This behaviour is similar to that of a linear system.

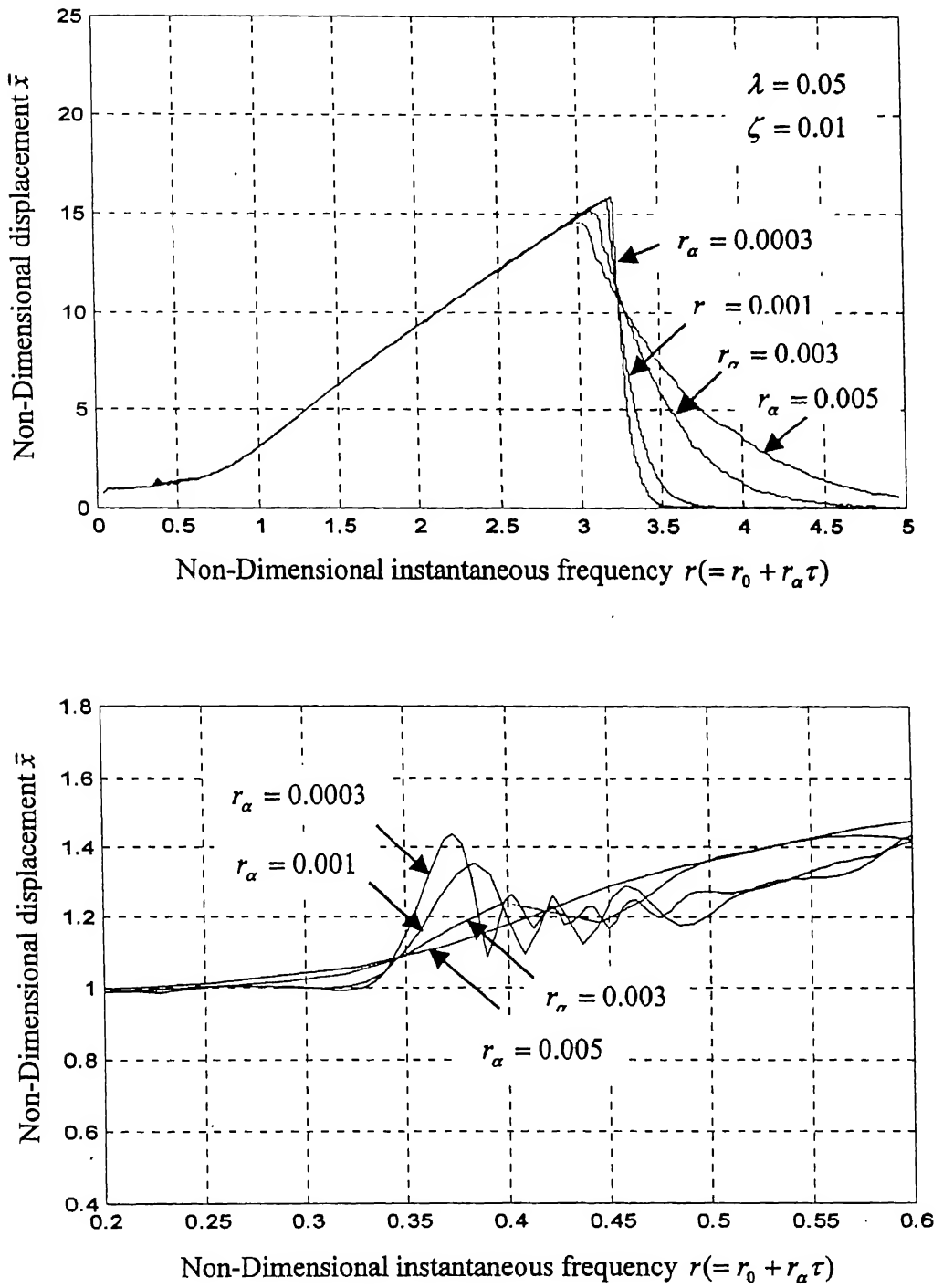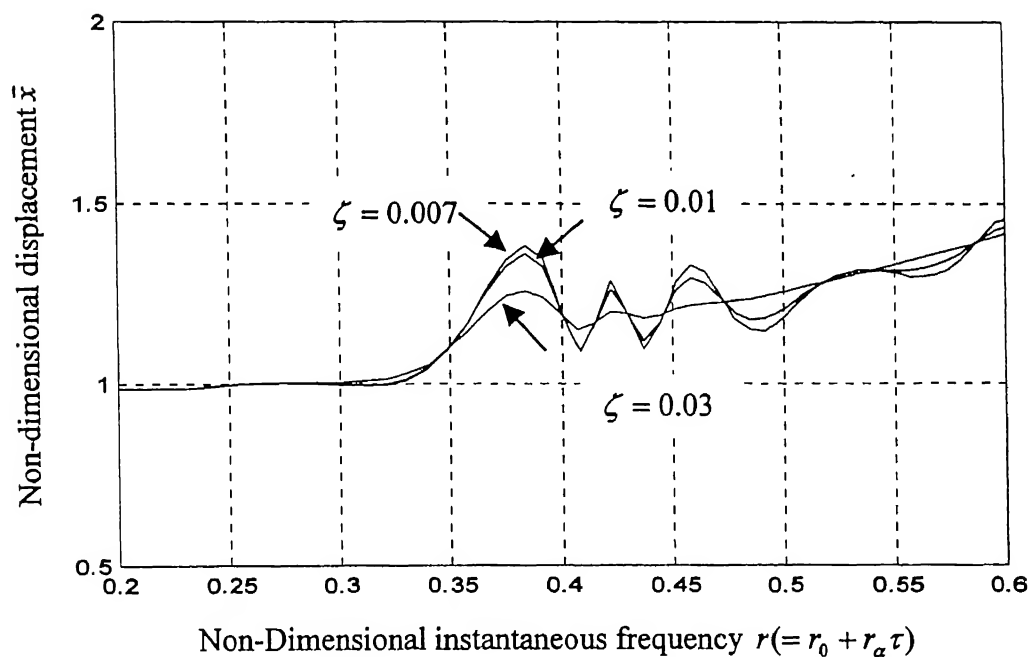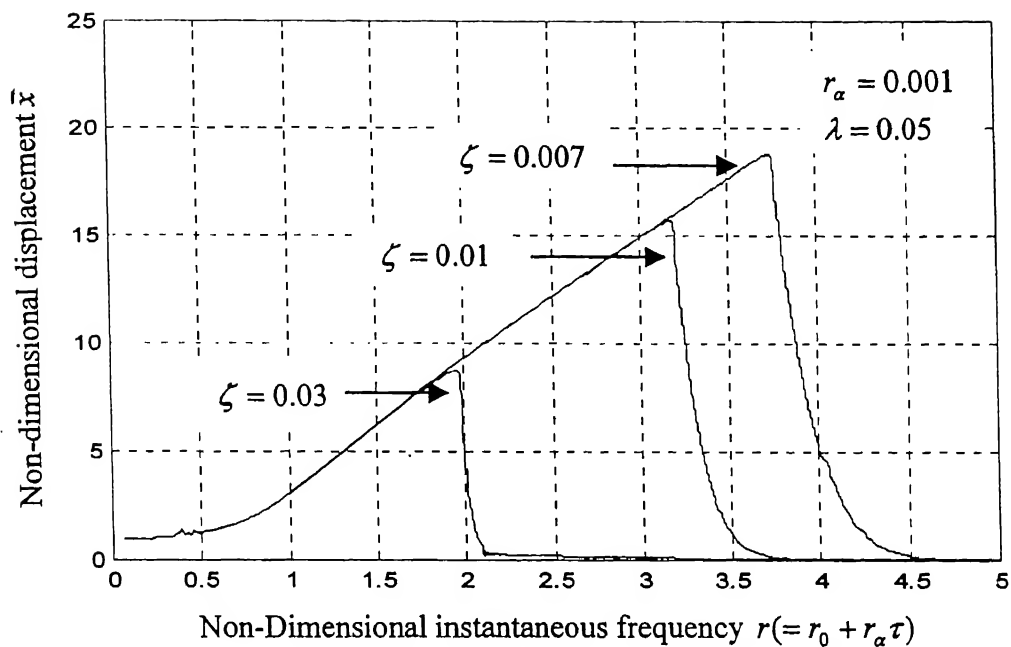(b) The resonance curves are not symmetric as in linear systems. The response during positive acceleration is starkly different than that during negative acceleration.

(c) The nonstationary response of a nonlinear system is associated with a jump phenomenon. The jump is steeper, when the rate of acceleration is less.

(d) Higher nonlinearity results in lower values of the maximum response achieved during positive acceleration The shift in the apparent resonant point is higher for higher magnitudes of the nonlinearity parameter λ, during positive acceleration, while for negative acceleration the apparent shift of the resonant point towards left is less for higher values of λ. This is in accordance with the fact that for higher nonlinearity, the bent of the backbone curve to the right of $r = 1$, is more pronounced.

(e) A phenomenon exactly opposite to that described in (d) above, takes place when the spring is soft (negative λ).

(f) The nonstationary response is also characterised by the presence of transient 1/3 subharmonic. The subharmonic also undergoes an apparent shift, depending on the magnitude and sign of nonlinearity as well as the magnitude and sign of the acceleration rate.

(g) The influence of linear damping, as expected, is a reduction in vibratory amplitude.

Comparison with Asymptotic Method

The numerically simulated results have been compared with those obtained through the Asymptotic Method proposed by Krylov and Bogolyubov (1956) through their method of asymptotic expansions. This has been done in order to check the correctness of the numerical simulations. A brief description of the asymptotic method is given below.

Writing a general governing equation for a non-linear single degree of freedom system as

$$\ddot{x} + p^2 x = \varepsilon f(x, \dot{x}) \tag{3.10}$$

21

where $p = \sqrt{k/m}$ is the linear natural frequency and ε is a small parameter, the purely harmonic response for the case when $\varepsilon = 0$, is

$$x = a \cos \psi \tag{3.11}$$

with a constant amplitude a and uniform rotating phase angle ψ, i.e.

$$\dot{a} = 0 , \quad \dot{\psi} = \omega \tag{3.12}$$

The existence of nonlinear perturbation ($\varepsilon \neq 0$), results in the appearance of overtones in the solution of equation (3.10). It also establishes dependence between the instantaneous frequency $\dot{\psi}$ and the amplitude a, and finally gives rise to systematic increase or decrease in the amplitude of the vibrations, depending upon whether the energy is expelled or absorbed by the perturbing force. Taking all these into account a general solution is sought in the form of expansion

$$x = a \cos(\psi) + \varepsilon u_1(a, \psi) + \varepsilon^2 u_2(a, \psi) + \dots + \varepsilon^m u_m(a, \psi) \quad m = 1, 2, \dots \tag{3.13}$$

where $u_1(a, \psi), u_2(a, \psi)$ are periodic functions of the angle ψ with period 2π and the quantities a, ψ, as function of time, are defined by the differential equations

$$\dot{a} = \varepsilon A_1(a) + \varepsilon^2 A_2(a) + \dots + \varepsilon^m A_m(a) \tag{3.14}$$

$$\dot{\psi} = \omega + \varepsilon B_1(a) + \varepsilon^2 B_2(a) + \dots + \varepsilon^m B_m(a)$$

Thus, the problem of constructing asymptotic approximations for equation (3.10) reduces to the choice of suitable expressions for the functions $u_1(a, \psi), u_2(a, \psi) \dots, A_1(a), A_2(a) \dots, B_1(a), B_2(a) \dots$ in such a way that equation (3.13) would, after replacing a and ψ by the functions of time defined by equation (3.14), serve as a solution of the initial equation (3.10). The practical applicability of asymptotic method is known to be determined not by the convergence properties of the series (3.13) and (3.14) when $m \to \infty$, but by their asymptotic properties for a given fixed value of m when $\varepsilon \to 0$. Applying the above method to the cubic non-linear case under present consideration (equation reproduced below)

22

$$m\ddot{x} + c\dot{x} + k_1 x + k_3 x^3 = f_0 \sin(\omega_0 t + \frac{1}{2}\alpha t^2) \tag{3.15}$$

and further rendering it in nondimensional form as

$$\bar{x}'' + 2\zeta\bar{x}' + \bar{x} + \bar{x}^3 = \gamma \sin(r_0\tau + \frac{1}{2}r_a\tau^2) \tag{3.16}$$

with

$$\tau = pt \qquad\qquad r_0 = \omega_0/p \qquad\qquad r_a = \alpha/p^2$$

$$\bar{x} = \left(\sqrt{k_3/k_1}\right)x \qquad \bar{x}' = \left(\sqrt{k_3/k_1}\right)x' \qquad \bar{x}'' = \left(\sqrt{k_3/k_1}\right)x''$$

$$2\zeta = c/mp \qquad\qquad \gamma = x_{st}\sqrt{k_3/k_1}\,. \qquad p = \sqrt{k_1/m}$$

the first approximation of the response is

$$x = a\cos(\theta + \phi) \tag{3.17}$$

with

$$\dot{a} = -\zeta a - \frac{\gamma}{1+\nu}\cos(\phi) \tag{3.18}$$

$$\dot{\phi} = 1 - \nu + 3\frac{a^2}{8} + \frac{\gamma}{a(1+\nu)}\sin(\phi)$$

The second approximation can be shown to be (Evan-Iwanowski ,1976)

$$x = a\cos(\theta + \phi) + \frac{a^3}{32}\cos 3(\theta + \phi) \tag{3.19}$$

with

$$\dot{a} = -\zeta a + \frac{3a^3\zeta}{8} - \gamma\left(\frac{1}{1+\nu} - \frac{3a^2(7-\nu)}{8(3-\nu)(1+\nu)^2}\right)\cos(\phi)$$

$$+ \gamma\left(\frac{1}{(1+\nu)^3}\dot{\nu} - \frac{\zeta}{(1+\nu)^2}\right)\sin(\phi) \tag{3.20}$$

$$\dot{\phi} = 1 - \nu + \frac{3a^2}{8} - \frac{\zeta^2}{2} - \frac{15a^4}{256} + \frac{\gamma}{a}\left(\begin{array}{l}\left(\dfrac{1}{1+\nu} - \dfrac{3a^2(5-3\nu)}{8(3-\nu)(1+\nu)^2}\right)\sin(\phi) \\[2mm] + \left(\dfrac{1}{(1+\nu)^3}\dot{\nu} - \dfrac{\zeta}{(1+\nu)^2}\right)\cos(\phi)\end{array}\right)$$
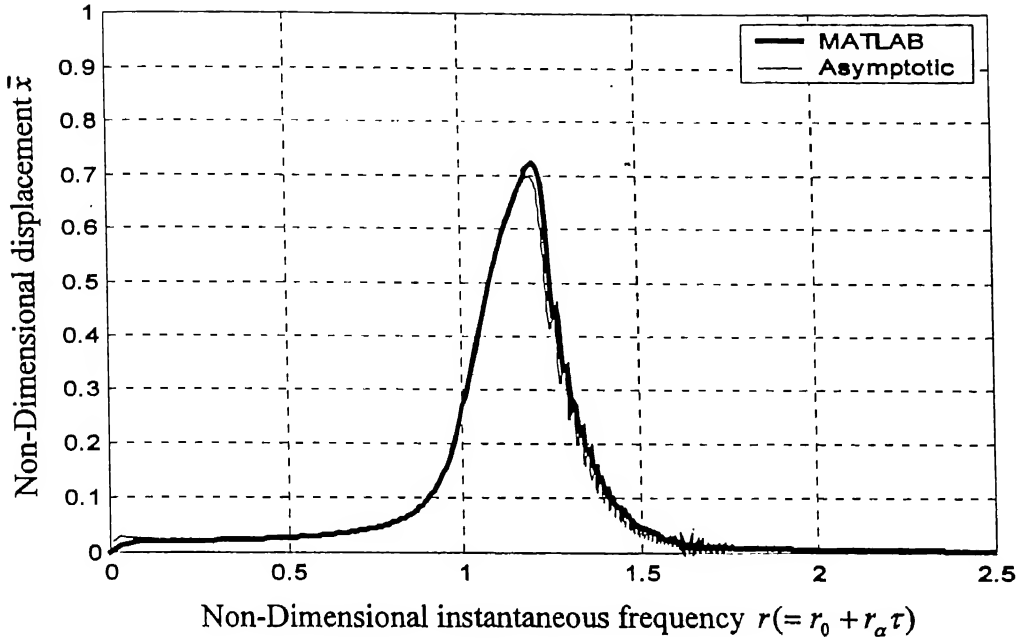
Fig. 3.6   Response comparison of simulation and asymptotic method

The results with the second approximation (equations 3.19, 3.20) for $r_\alpha = 0.001, \zeta = 0.01$, and $\gamma = 0.03$ are shown in Fig 3.6. The numerical results obtained through the fourth order Runge-Kutta model in MATLAB are also shown in the figure. The good qualitative and quantitative closeness between the two sets of curves is taken as a measure of the correctness of the numerical model developed in MATLAB.

3.1.2   Case (2):Combined Square and Cubic nonlinearity($k_1 \neq 0$, $k_2 \neq 0$, $k_3 \neq 0$)

A system with both square and cubic stiffness nonlinearity is considered next. The governing equation with linear damping and a sinusoidal excitation force with frequency constantly increasing with time can be written as,

$$m\ddot{x} + c\dot{x} + k_1 x + k_2 x^2 + k_3 x^3 = f_0 \sin(\omega_0 t + \frac{1}{2}\alpha t^2) \tag{3.21}$$
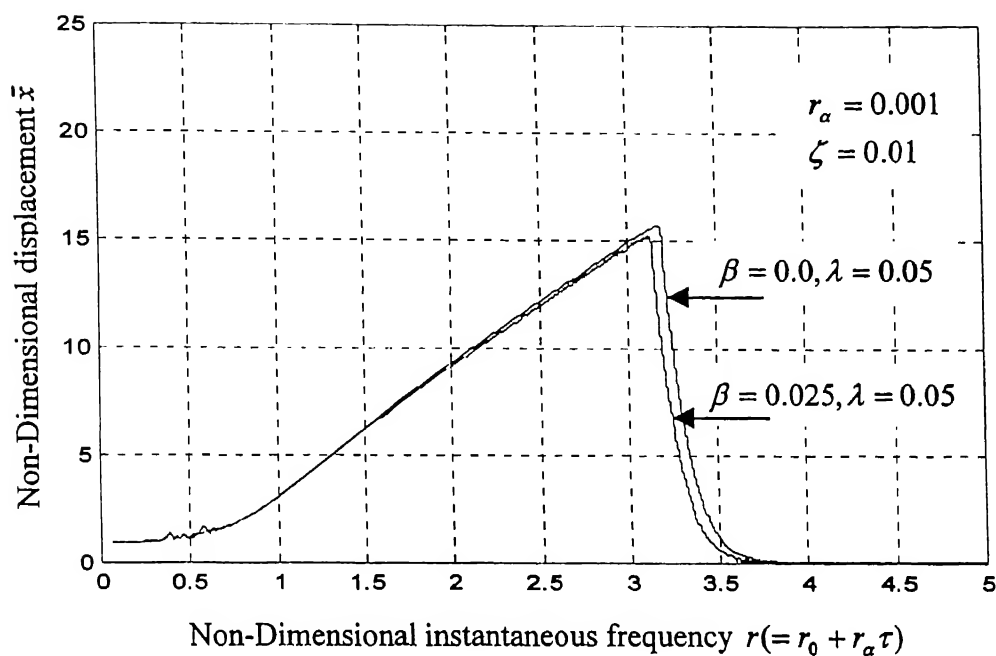
24

Fig. 3.7(a)   Non-stationary response of square-cubic and cubic nonlinear systems
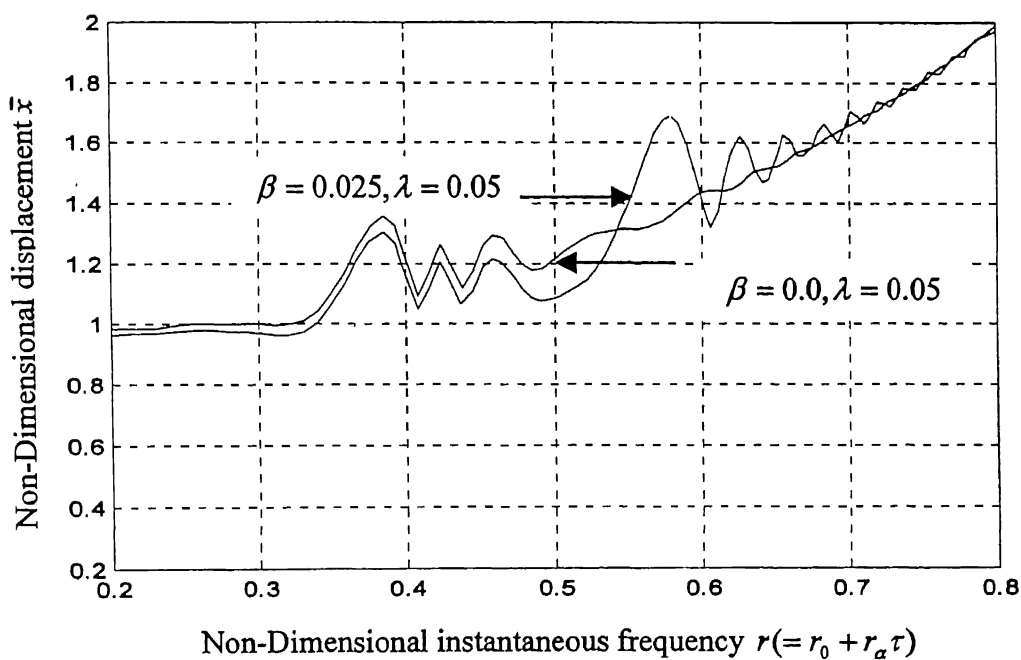

Fig. 3.7(b)   Subharmonics for combined square-cubic and cubic nonlinearity
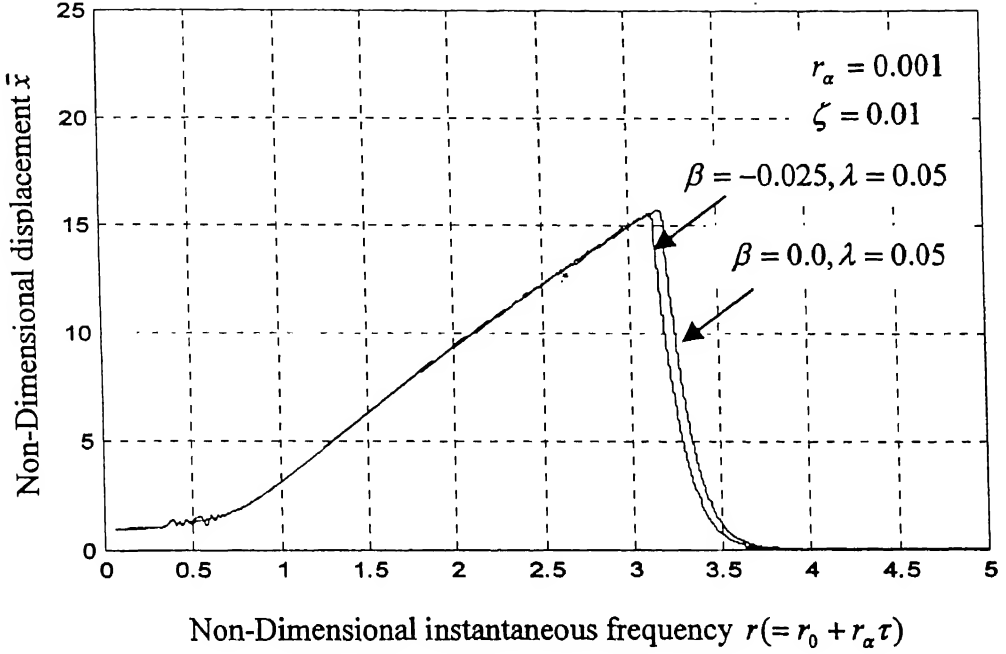
Fig. 3.7(c)   Non-stationary response of square-cubic ($\beta < 0, \lambda > 0$)

and cubic nonlinear systems

Employing the parameters defined in equation (3.13 a) and $\beta = k_2 f_0 / k_1^2$, equation (3.21) can be written in nondimensional form as,

$$\bar{x}'' + 2\zeta\bar{x}' + \bar{x} + \beta\bar{x}^2 + \lambda\bar{x}^3 = \sin(r_0\tau + \frac{1}{2}r_\alpha\tau^2) \qquad (3.22)$$

The MATLAB Simulink model for numeric solution of equation (3.22) is given in Appendix 3. The nondimensional response of the system is shown in Fig 3.7(a), for a nonstationary case, with acceleration, $r_\alpha = 0.001$. It can be seen that the presence of square nonlinearity, β, causes $r/2$ subharmonic resonance. This subharmonic has been zoomed in Fig. 3.7 (b). Other characteristics appear similar to a cubic nonlinear system. Fig 3.7 (a) corresponds to a positive value of β (=0.025), while in Fig 3.7(c) the response corresponds to a negative value of β (= -0.025). In both cases the value of cubic

26

nonlinear parameter λ and rate of acceleration r_a were kept constant at 0.05 and 0.001 respectively. The figures also show comparison with the response of a purely cubic system (β = 0). It can be noted from Figs. 3.7 a, c that a positive value of β, results in downward shift of the response curve in comparison with that of a purely cubic system. A negative value of β causes the opposite. (This fact can be understood by transforming equation (3.21) into an alternative form $m\ddot{q} + c\dot{q} + a_1 q + a_3 q^3 = f_0 \sin(\omega_0 t + \alpha t^2 / 2) + f_{dc}$;

with $q = x + \dfrac{k_2}{3k_3}$; a_1, a_3, f_{dc} being constants depending upon k_1, k_2 and k_3; and carrying

out further analysis as suggested by Hayashi, (1964).

3.2 Symmetric Square Nonlinearity

A system with nonlinear restoring force $g(x) = x|x|$ is considered here. The governing equation is written as

$$m\ddot{x} + c\dot{x} + kx \mid x \mid = f_0 \sin(\omega_0 t + \frac{1}{2}\alpha t^2) \tag{3.23}$$

and in nondimensional form as

$$\bar{x}'' + 2\zeta\bar{x}' + \bar{x} \mid \bar{x} \mid = \sin(r_0 \tau + \frac{1}{2}r_a \tau^2) \tag{3.24}$$

where $p^2 = kx_0/m$; $x_0^2 = f_0/k$ (other parameters same as defined in equation 3.13 a)

The Simulink model developed for the purpose is shown in Appendix 4. Fig 3.8 shows the response characteristics of equation (3.24) for acceleration and deceleration rate r_a = 0.001. The response is characterised by the presence of both 1/3 and 1/2 subharmonics. Explanation of this behaviour can be attempted by expressing the restoring force $g(x) = x|x|$, by an equivalent polynomial power series form of the type given by equation (3.2) i.e. $g(x) = k_1 x + k_2 x^2 + k_3 x^3 + \ldots\ldots\ldots$. It is to be noted here, that the equivalent terms k_1, k_2, k_3 will be dependent on the response level x. If the curve fitting is carried out over the entire range of the maximum response level ($-14 \le x \le 14$) of Fig.3.8 the following values of equivalent terms are obtained,
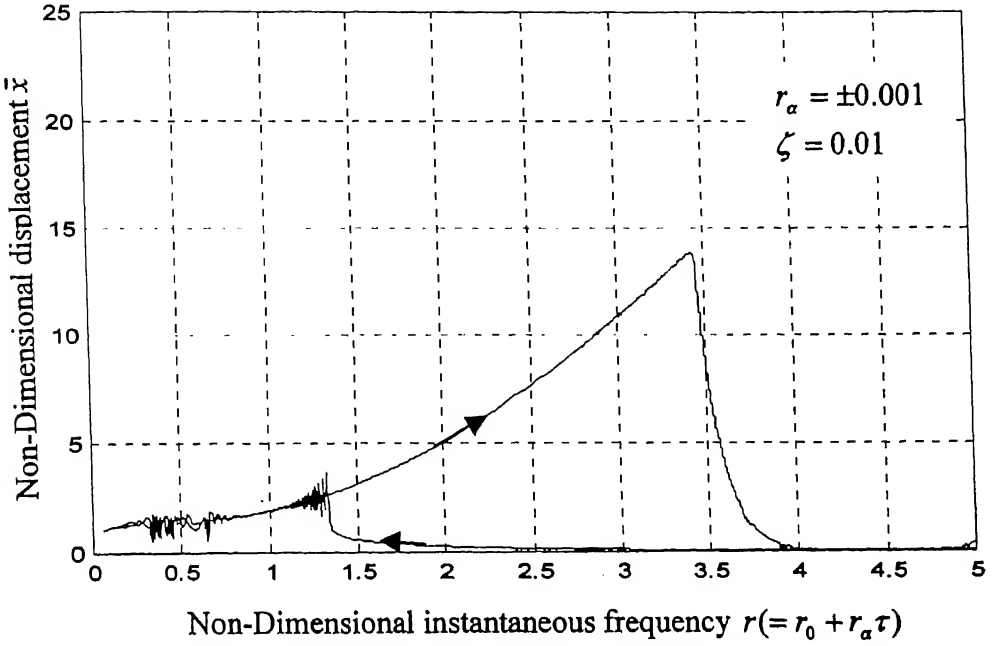
$r_\alpha = \pm 0.001$

$\zeta = 0.01$

Fig. 3.8   Response of symmetric square system during acceleration and deceleration

$k_1 = 4.3904$

$k_2 = 0.0$ (3.25)

$k_3 = 0.0519$

Fig. 3.9 gives a comparison of the actual square symmetric spring force and that obtained by the equivalent polynomial representation. Fig. 3.10 shows a comparison between the behaviour of the system with actual nonlinear function $g(x) = x|x|$ and that with equivalent polynomial form function $g(x) = k_1 x + k_2 x^2 + k_3 x^3$, with values as given above in equation (3.25). The curves have been obtained for acceleration rate $r_\alpha = 0.001, \zeta = 0.01$.While the equivalent polynomial approximates the symmetric square nonlinearity closely in the resonance zone, it misses out on depicting the subharmonics. However, if the curve fitting to obtain the equivalent polynomial form is restricted to the response
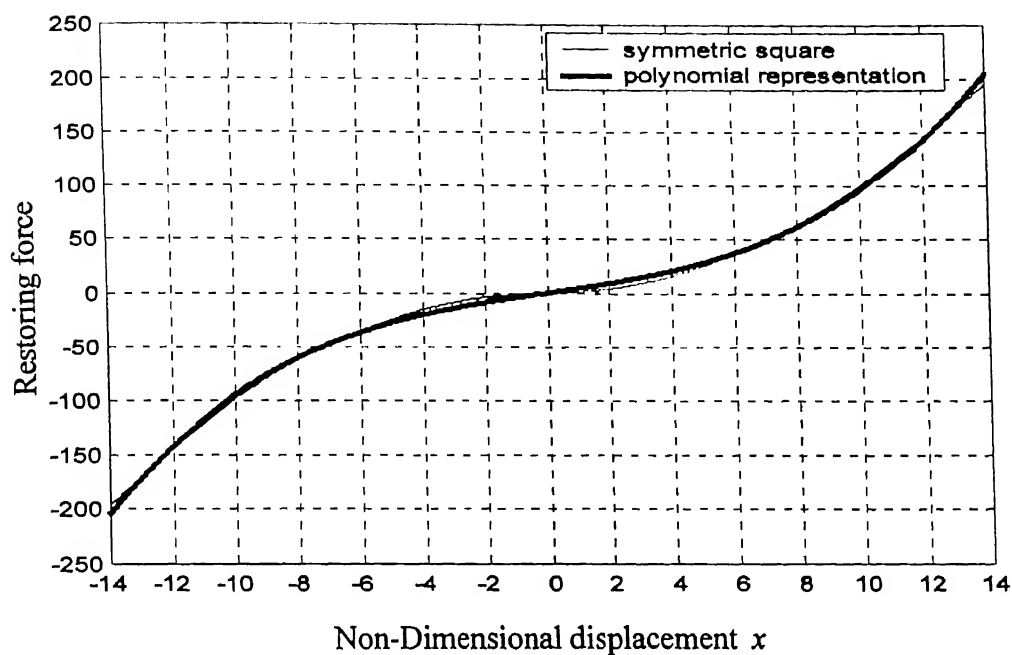
Fig. 3.9 Square symmetric ($x|x|$) and equivalent polynomial spring force
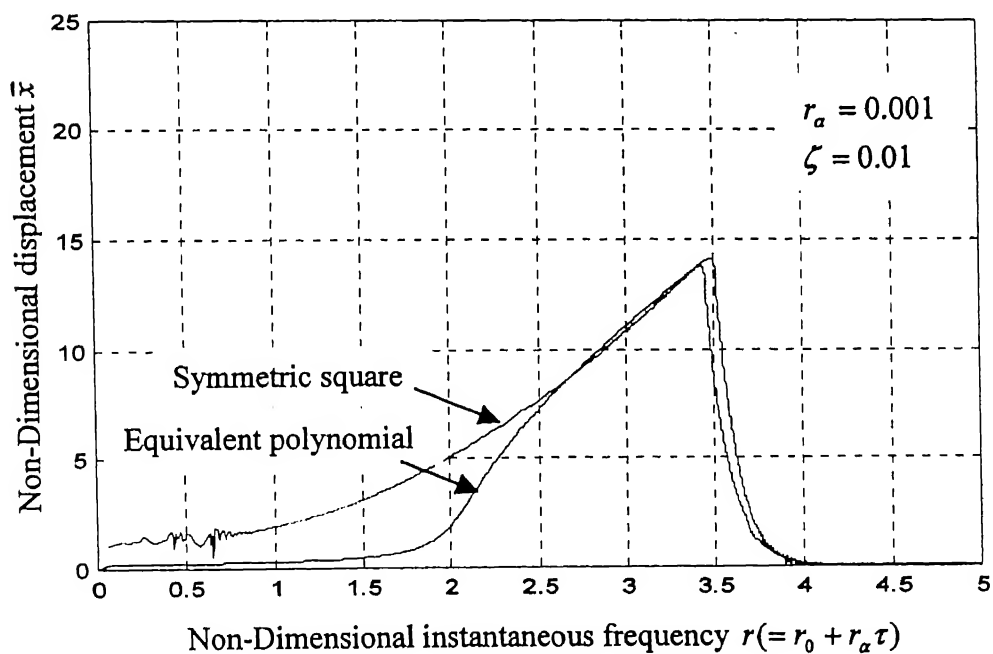

Fig. 3.10 Comparison of square symmetric $x|x|$ and equivalent polynomial system response
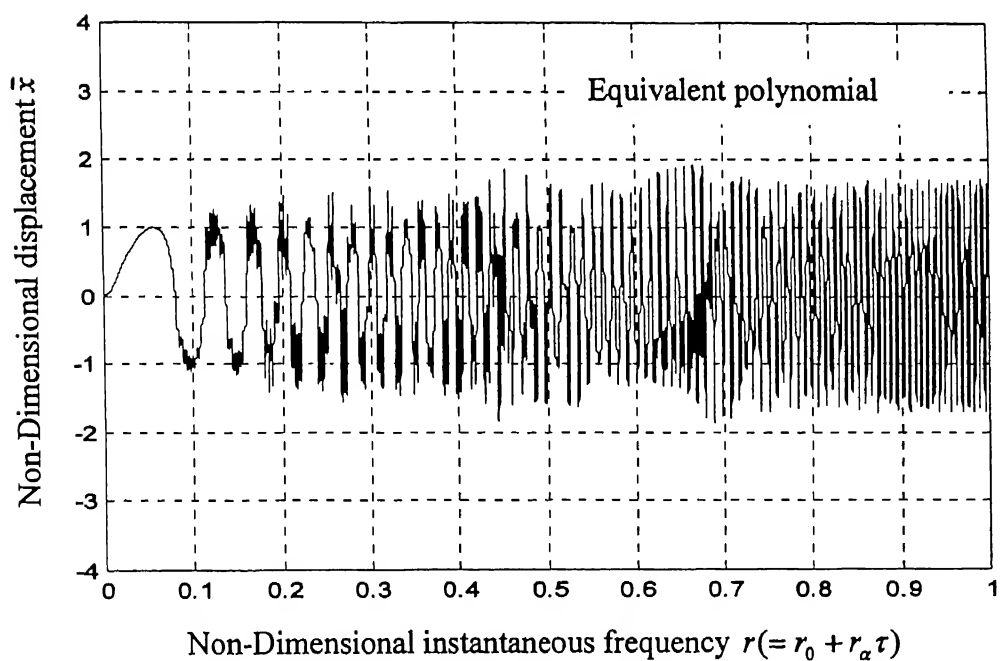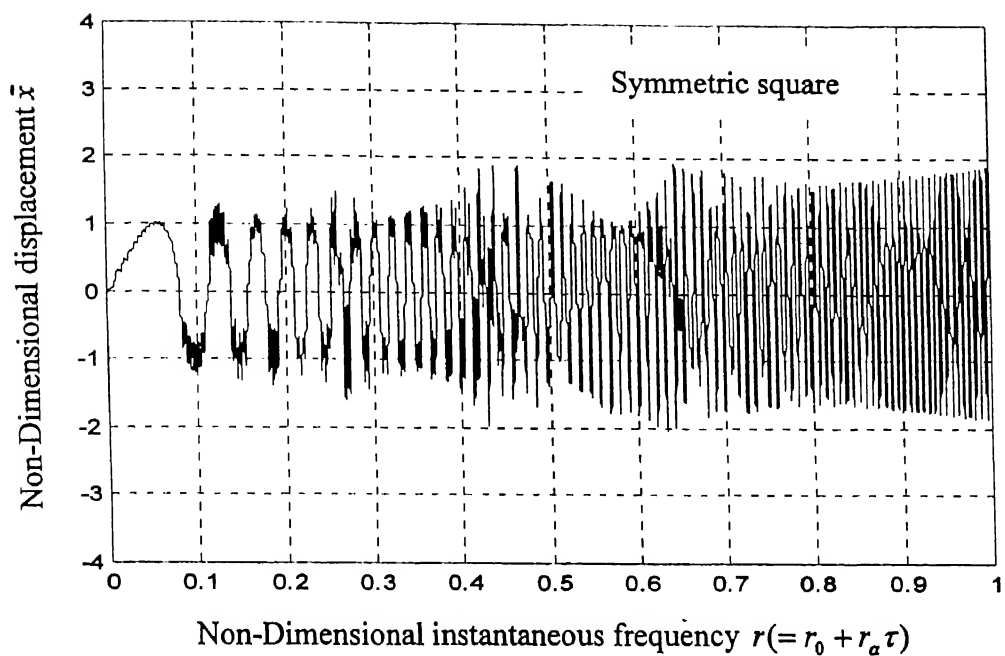
29

Fig. 3.11   Subharmonics of square symmetric $x \mid x \mid$ system and equivalent

polynomial form

level in the subharmonic zone $(-2 \leq x \leq 2)$ the values of coefficients of equivalent power series, come out to be,

$$k_1 = 0.6265$$

$$k_2 = 0.0$$

$$k_3 = 0.3638$$

The response behaviour for this polynomial approximation (Fig.3.11) can now be seen to reflect the subharmonic response characteristics of the $x \mid x \mid$ system, quite correctly.

3.3   Bearing Nonlinearity

Most rotors are supported in oil-film or in rolling element bearings. The bearings influence the rotor vibrations to greater or less degree by their dynamic properties in comparison to those of the rotor and the remaining components of the assembly. This influence originates essentially from the ratio of rotor stiffness to bearing stiffness. For a relatively elastic rotor the influence of the bearings is small while dynamics of a stiff rotor are determined by the bearings. A typical case of a rigid rotor in rolling element bearings with sinusoidal exciting force accelerating linearly with time is considered. The force-deflection relationship for a ball-bearing is generally expressed as, (Kramer, 1993)

$$g(x) = kx^{3/2}$$

$$= kx \mid x \mid^{1/2}$$

and the governing equation of the system as,

$$m\ddot{x} + c\dot{x} + kx \mid x \mid^{1/2} = f_0 \sin(\omega_0 t + \frac{1}{2}\alpha t^2) \tag{3.26}$$

In nondimensional form (with $x_0^{3/2} = f_0/k$, in addition to the previously defined parameters), the governing equation becomes

$$\bar{x}'' + 2\zeta\bar{x}' + \bar{x} \mid \bar{x} \mid^{1/2} = \sin(r_0\tau + \frac{1}{2}r_a\tau^2) \tag{3.27}$$

The Simulink model for numerical solution of above equation is shown in Appendix 5. Fig 3.12 shows the response of accelerating and decelerating case ($r_a = 0.001$) and
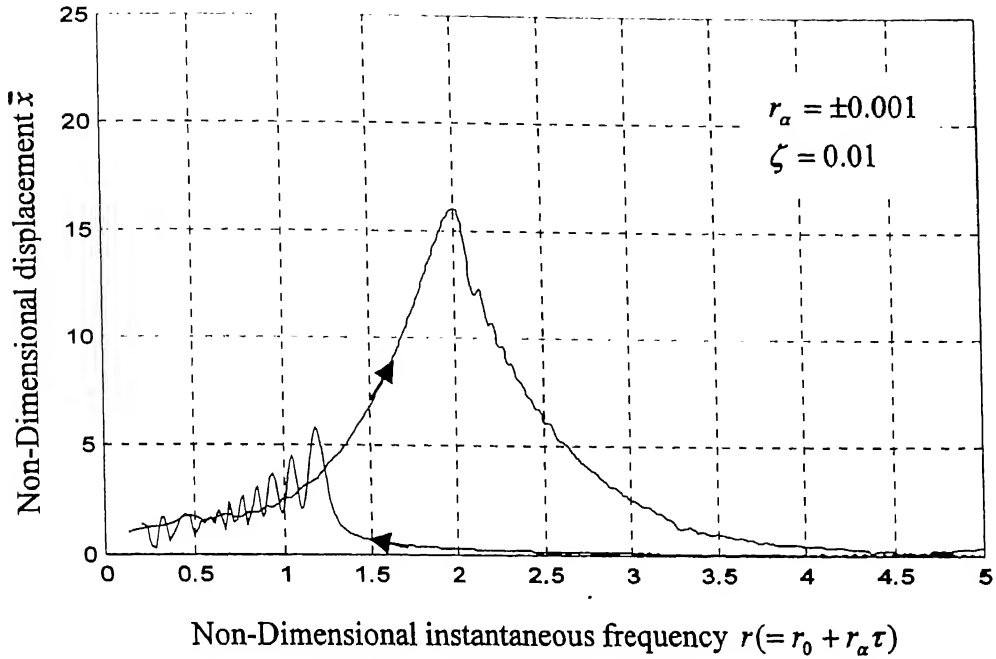
Fig. 3.12   Response for nonlinear bearing system

damping coefficient ζ =0.01. The apparent shift in resonance, in this case can be seen to be less than that of the symmetric square case (Fig.3.8). The influence of various acceleration and decceleration on the response patterns are shown in Figs. 3.13 (a), (b). Comparison with equivalent polynomial forms (Figs. 3.14, 3.15) reveal that other features, including the subharmonic phenomenon also show trends similar to that of square symmetric nonlinearity.
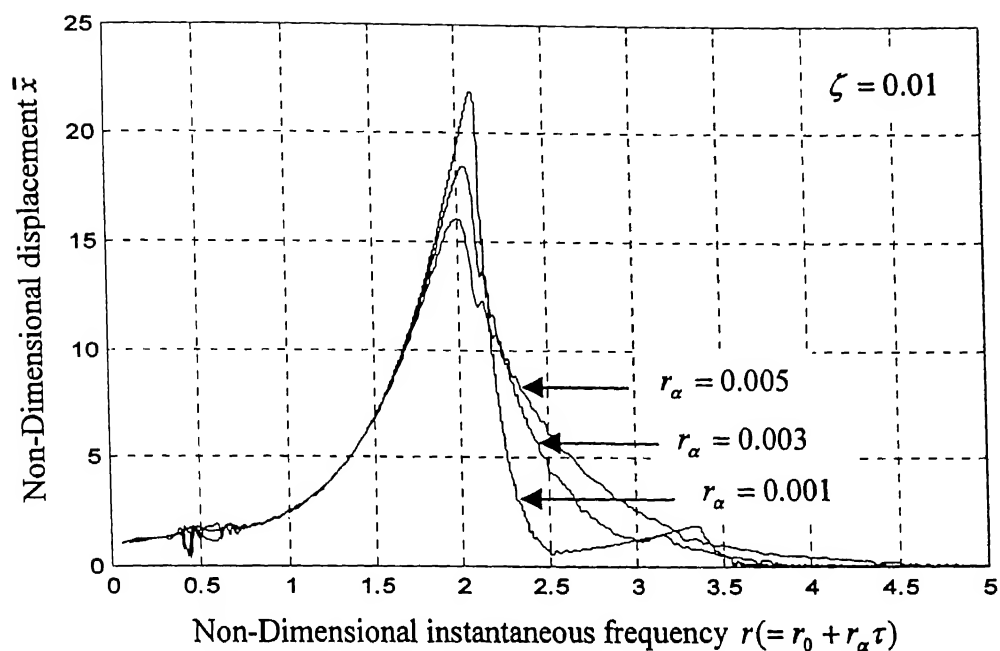
Fig. 3.13(a)   Influence of acceleration on nonlinear bearing system
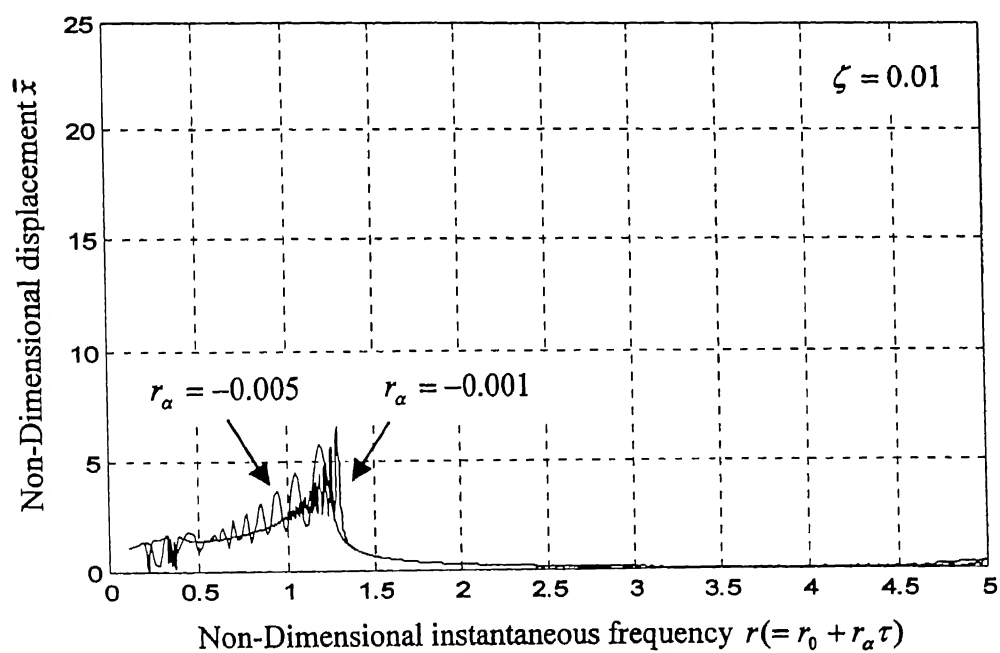

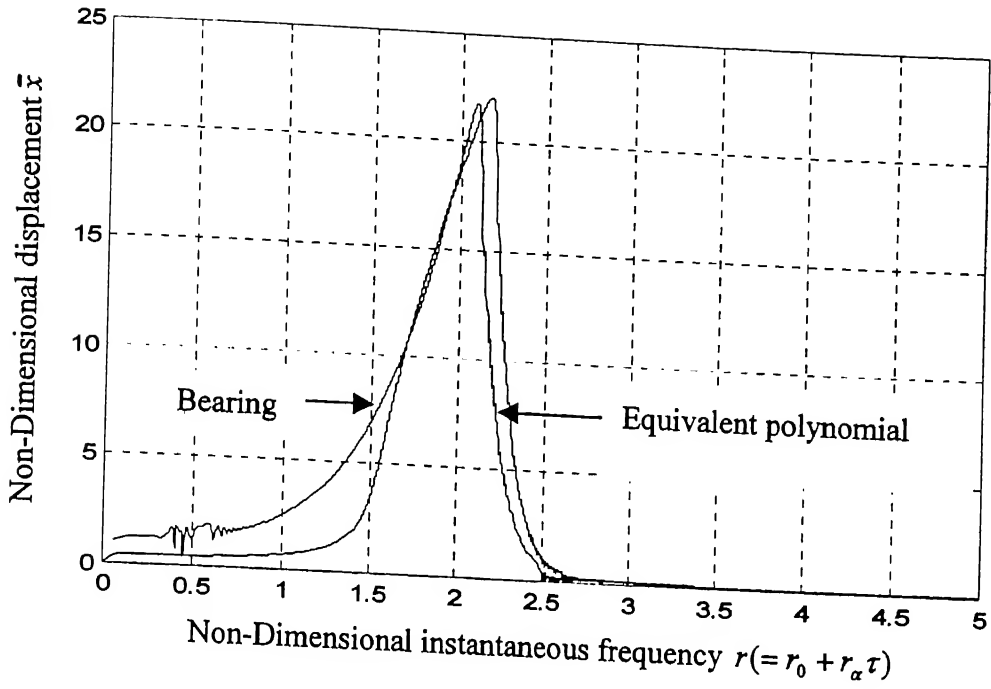**Fig. 3.13(b)   Influence of deceleration on nonlinear bearing system**

33

Fig. 3.14   Comparison of bearing non-linearity $x \, |x|^{1/2}$ and equivalent
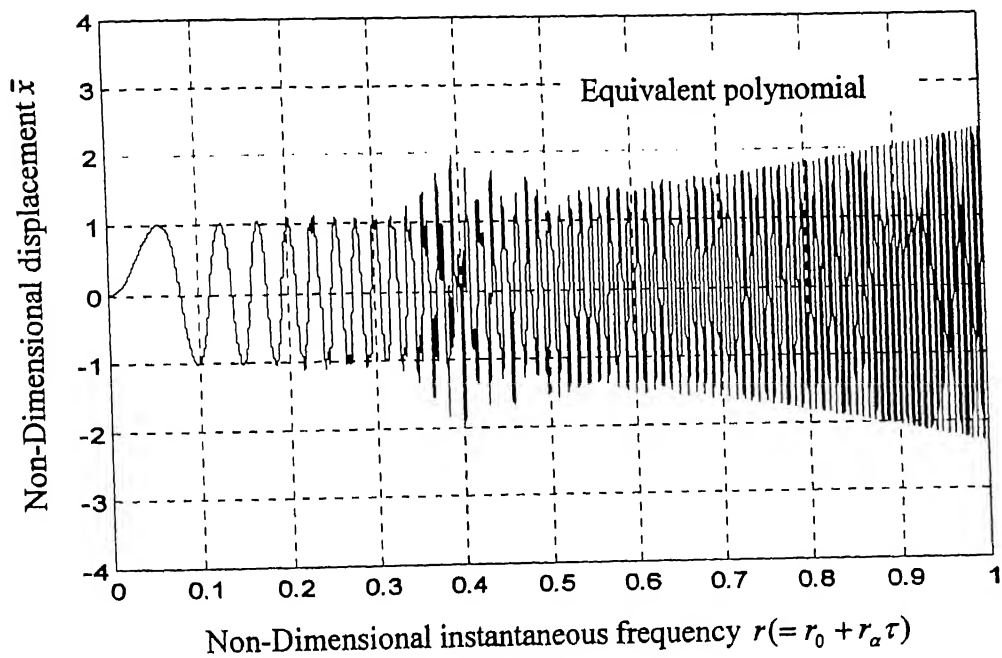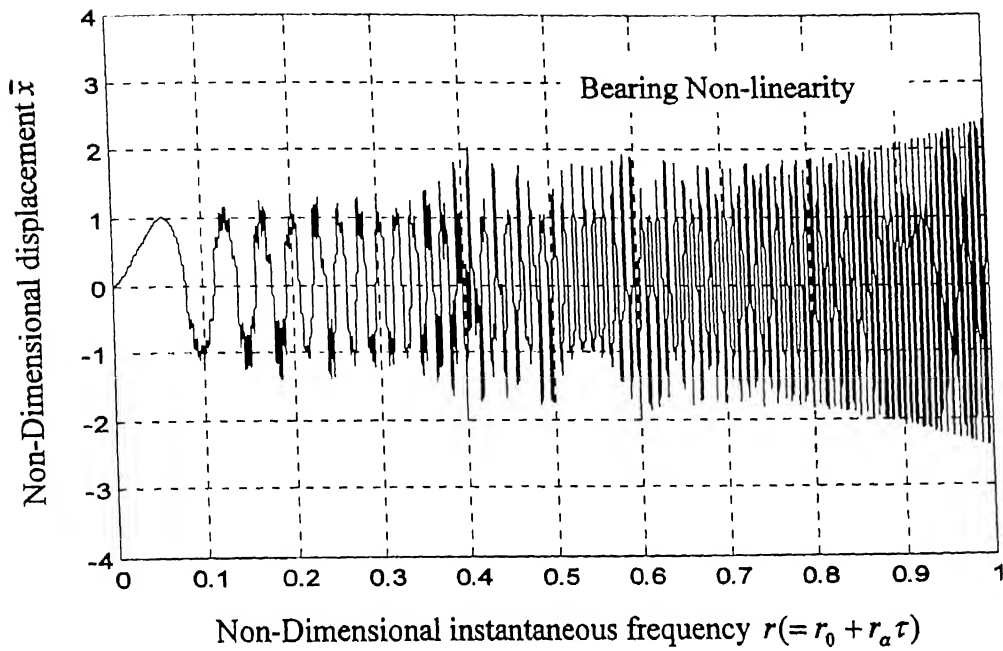polynomial system

Fig. 3.15 Subharmonics of nonlinear bearing system and equivalent polynomial form

3.4   Bilinear Nonlinearity

It is customary to represent fatigue cracks in structural members subjected to repeated loading through Breathing Crack models. A breathing crack is an idealisation to consider the change in stiffness of the structure (say, a beam), during vibration, when the crack is subjected to both tension and compression, during each cycle of vibration. The stiffness is less, when the crack is under tension and as a result the crack is open. The stiffness is higher and taken approximately equal to that of an uncracked beam, during that regime of the vibration cycle, when the crack is under compression and consequently closed. Such a system can be idealised through a bilinear governing differential equation given below.

$$m\ddot{x} + c\dot{x} + kx = f_0 \sin(\omega_0 t + 1/2\alpha t^2) \tag{3.29}$$

$$k = (1 - \varepsilon)k_1 \qquad\qquad\qquad \text{for } x > 0,$$

$$k = k_1 \qquad\qquad\qquad\qquad \text{for } x \leq 0,$$

Taking $p = \sqrt{k_1/m}$ (and the previously defined parameters), and writing the equation in nondimensional form

$$\bar{x}'' + 2\zeta\bar{x}' + (1 - \varepsilon)\bar{x} = \sin(r_0\tau + 1/2 r_\alpha\tau^2), \qquad \text{for } x \geq 0 \tag{3.30}$$

$$\bar{x}'' + 2\zeta\bar{x}' + \bar{x} = \sin(r_0\tau + 1/2 r_\alpha\tau^2) \qquad \text{for } x < 0$$

the response is numerically simulated through the Simulink model shown in Appendix 6. Fig 3.16 shows the response for the system under acceleration for different values of nondimensional bilinear stiffness ($(1-\varepsilon) = 0.999, 0.777$). With increase ($1-\varepsilon$), the system resonance is seen to shift away from $r = 1.0$. The figure also includes the curve under similar circumstances, for a purely linear case ($\varepsilon = 0$). The presence of bilinearity (due to say the presence of a crack) can be seen to result in higher amplitudes at resonance, which is as expected due to reduction in the system stiffness. With higher values of ε, the reduction in stiffness is more and consequently resonant amplitudes are higher. The response pattern, of the bilinear system, with different acceleration rates is shown in Fig. 3.17. The response of this system is also associated with the subharmonic phenomenon and explanation can be attempted through equivalent polynomial forms similar to the previous cases.
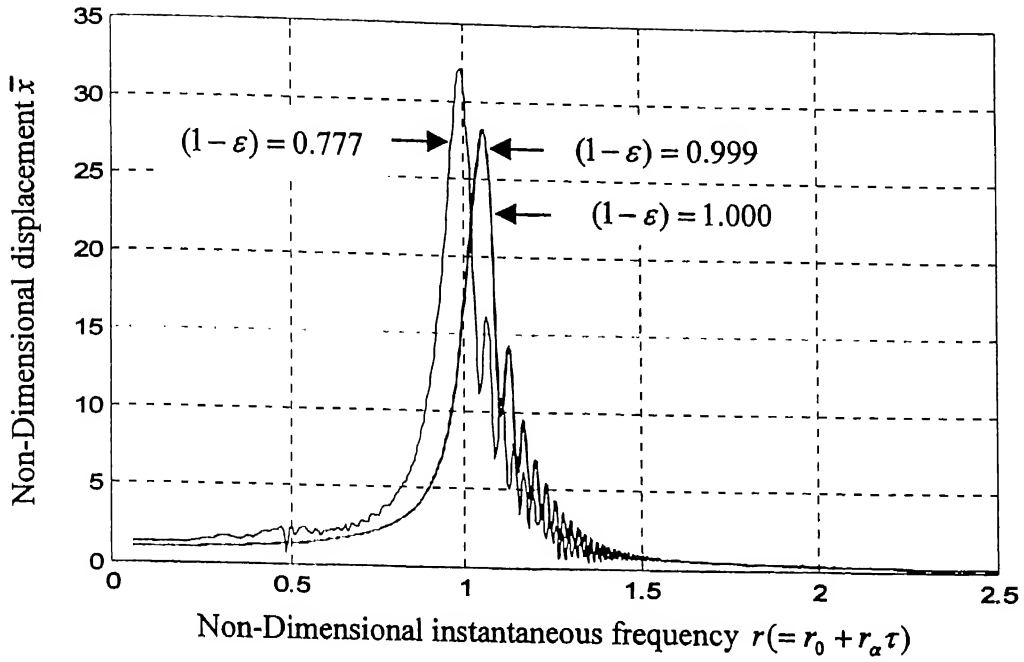
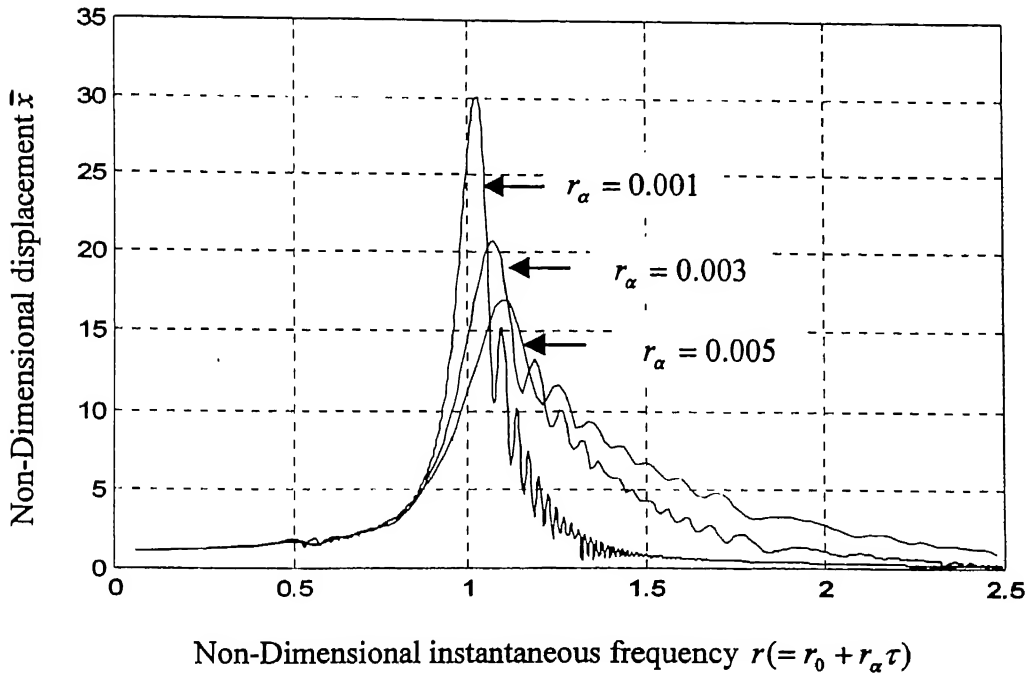**Fig. 3.16   Influence of bilinear stiffness during acceleration**

Fig3.17   Influence of acceleration rates (bilinear system)

37

CHAPTER 4

EXPERIMENTAL INVESTIGATIONS

Experimental investigations have been carried out for better understanding of the response patterns of a nonlinear system under a sweep test. The experiments were carried out on a readily available thin beam, which under large amplitudes of oscillation can exhibit nonlinear characteristics. The exercise was carried out with the aid of Virtual Instruments developed in the programming software LabVIEW.

4.1   Experimental Set-Up

The experimental set-up comprised a thin, commercially available ruler scale mounted on an electrodynamic shaker at one end (Fig.4.1). The beam approximately represented a cantilever configuration. However, since the vibrational modes were far separated, analysis could be carried out for the fundamental mode by treating the response to be similar to that of a single degree freedom system. The geometric and material properties of the beam are given below.

Length, l = 362 mm   *Width, w = 25 mm*   *Thickness, d = 1.68mm*

Modulus of Elasticity, E = 100 GPa   *Density,* ρ *= 7200* $\frac{kg}{m^3}$

4.2   Instrumentation

The instrumentation employed for the study is shown in Figs. 4.2. The response of the beam was picked up through a miniature accelerometer Type: 4374 Bruel & Kjaer, Charge Sensitivity: 0.153 pc/ms^{-2}, Voltage Sensitivity: 0.197 mv/ms^{-2}. The signal from the accelerometer was conditioned and amplified in a Charge Amplifier (Bruel & Kjaer, Type 2635). The excitation signal for the Electrodynamic Shaker was generated in a Pentium PC, using LabVIEW. LabVIEW is program development application, much like C or BASIC. However, LabVIEW uses graphical programming language, G, to
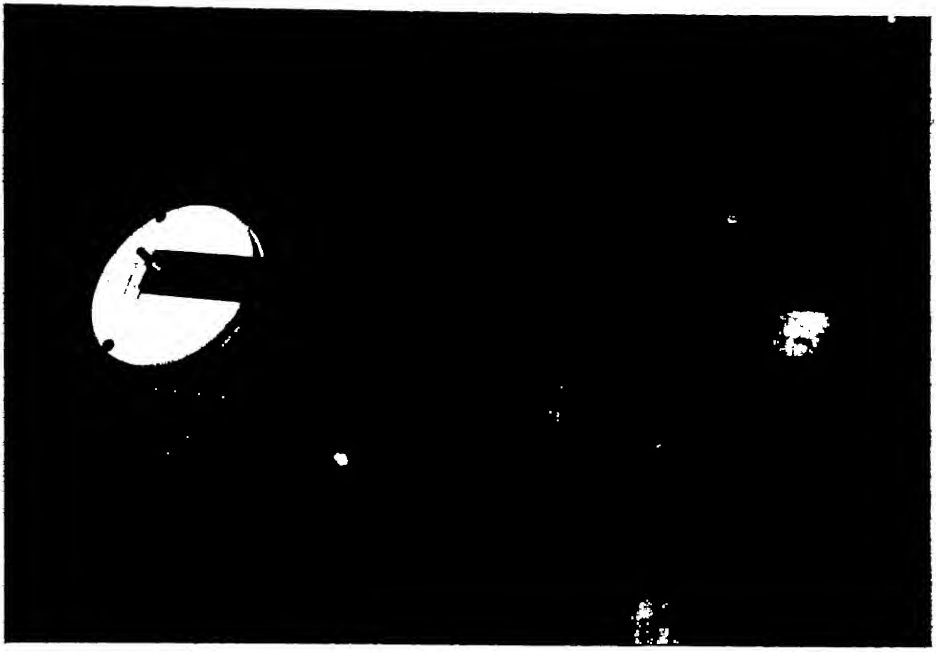
Fig .4.1   Specimen mounted on electrodynamic shaker

Fig. 4.2   Experimental set up.

create programs in block diagram form. In addition of having extensive libraries of functions, LabVIEW includes libraries for data acquisition, GPIB and serial instrument control, data analysis, data presentation, and data storage. The programs developed in LabVIEW are called virtual instruments (VI_s) because their appearance and operation can imitate actual instruments. Thus a VI consists of:

Front panel: The interactive user interface of the program is called front panel, because it simulates the panel of a physical instrument. The front panel can contain knobs, push buttons, graphs, and other controls and indicators. Data can be entered using mouse or keyboard.

Block Diagram: The block diagram is a pictorial solution to a programming problem. It is also the source code for the VI.

The Block Diagram developed, during the course of this study, for signal generation is shown in Fig. 4.3 (b). The Front Panel of the VI is shown in Fig.4.3 (a).
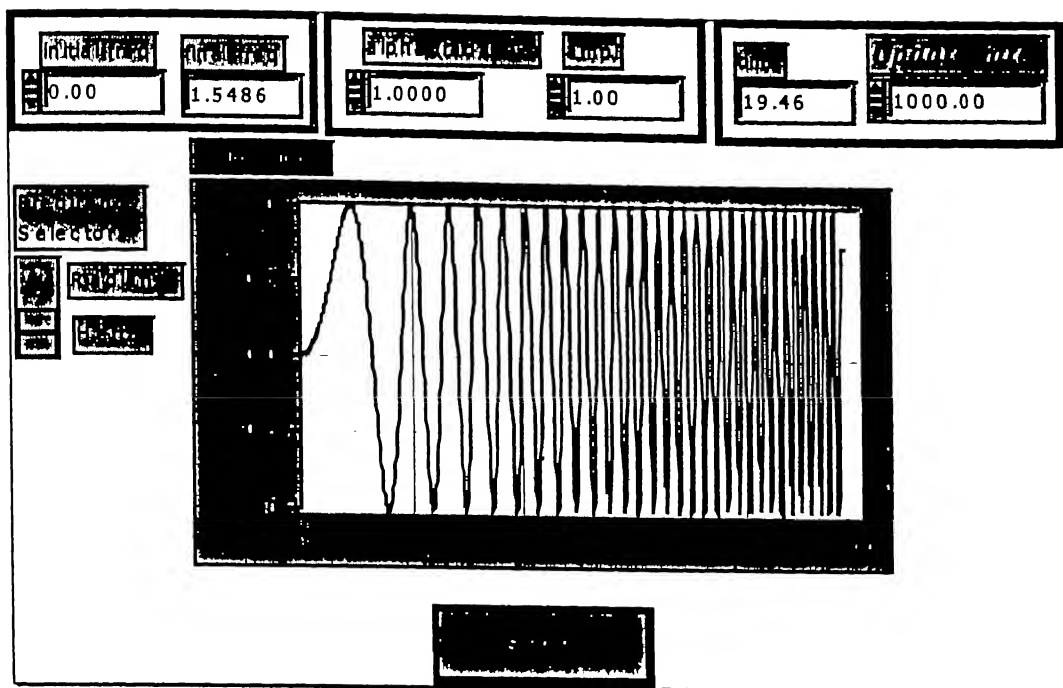
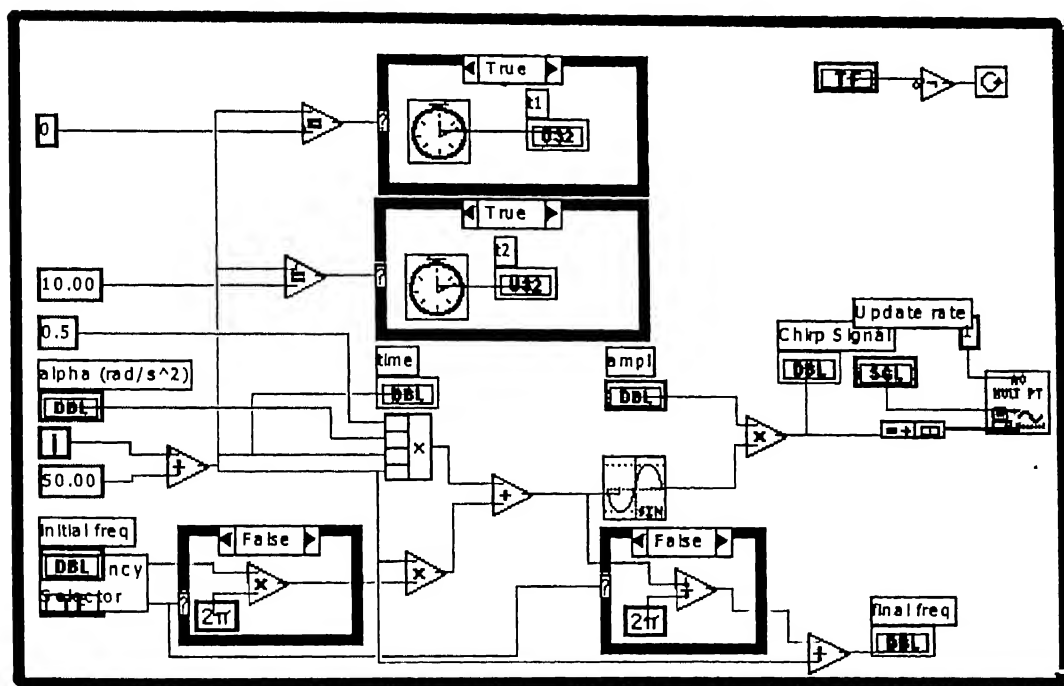Fig. 4.3(a)   Front panel of VI for signal generation

Fig. 4.3(b)   Block diagram of VI for signal generation

The Virtual Instrument can generate a sinusoidal signal with a time varying frequency. The initial frequency as well as the rate of change of frequency (positive or negative) can be set through the Front Panel of the VI. A software setting is also provided for the amplitude of the sinusoidal signal. The PC is equipped with an A/D card (National Instruments, Texas, AT-MIO-E16, with a scan rate of 250000 samples/s). The signal generated by the VI and coming out through the card is taken through an accessory (BNC 2090), which connects the A/D card to BNC type connectors, to a Power Amplifier (Type: SS250, MB Dynamics, Inc.) The output of the Power amplifier is fed to the electrodynamic shaker. The response signal is also taken to the computer, through the A/D card. The VI for data acquisition and display is shown in Figs. 4.4 (a), (b).
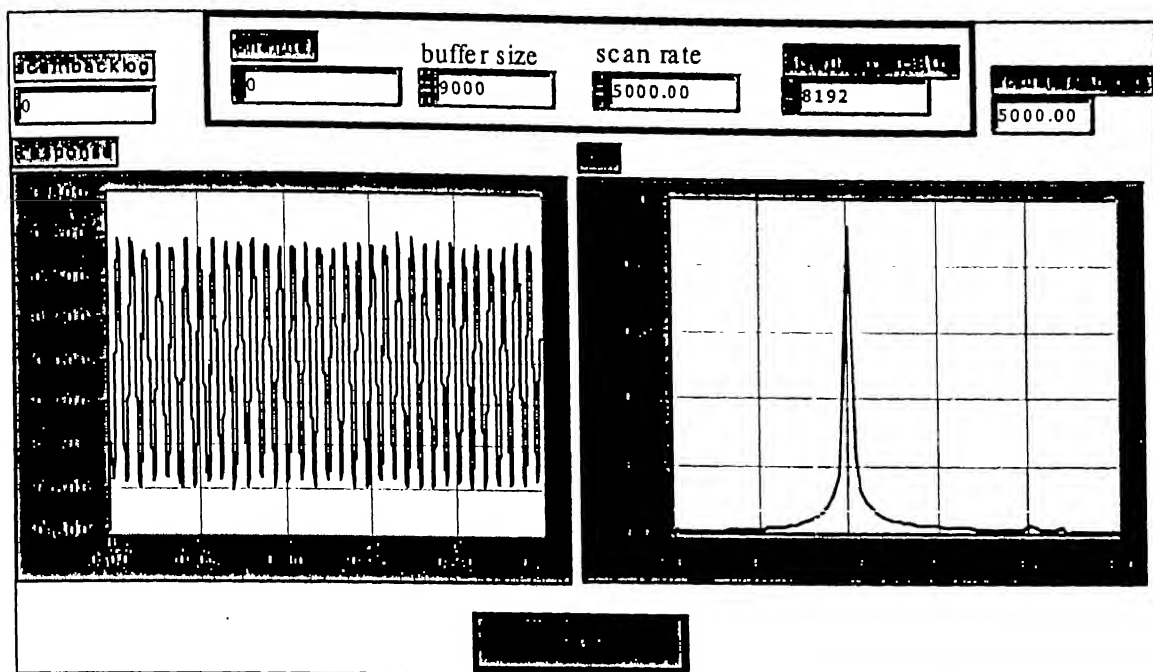
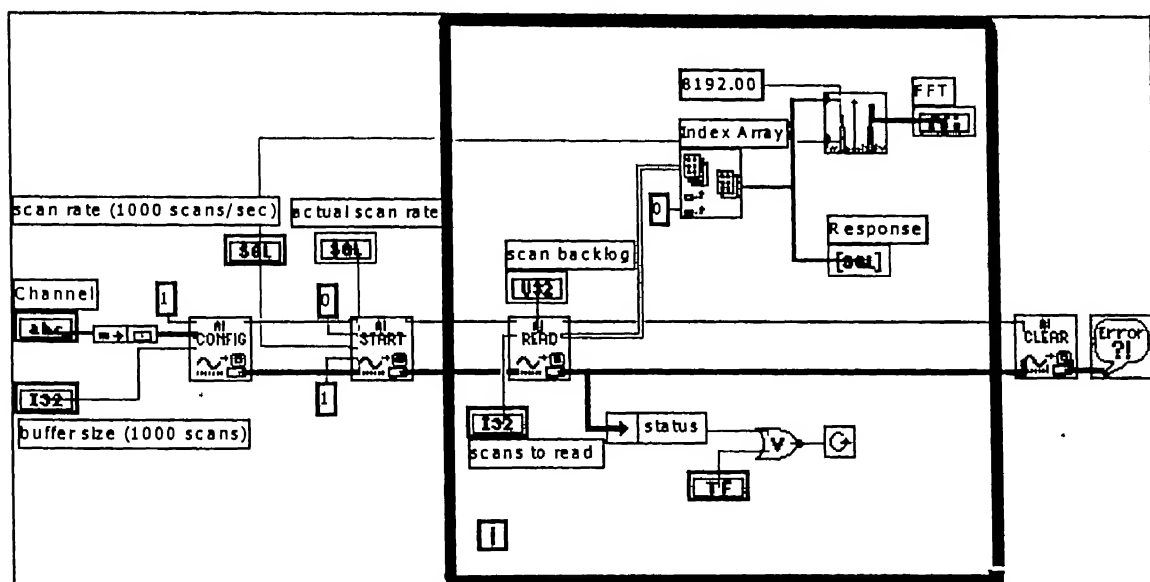**Fig. 4.4(a)   Front panel of VI used for Data Acquisition**

Fig. 4.4(b)   Block diagram of VI used for Data Acquisition.

4.3   Experimental Results

Prior to carrying out, nonstationary analysis, a Rap-Test was performed on the beam to identify its linear natural frequencies. The beam was very slightly perturbed (to keep the vibrations in the linear zone) at its free end and the resultant free vibrations were recorded. The FFT of this response is shown in Fig. 4.5, from which the first two natural frequencies can be seen as 7.68Hz and 47.22Hz. The natural frequency were calculated theoretically also, employing the formula

$$\omega_n = (\beta_i l)^2 \sqrt{\frac{EI}{\rho l^4}}$$

(4.1)

where for a cantilever configuration $\beta_i l = 3.52, 22$ giving,

$\omega_1 = 7.72$Hz

$\omega_2 = 48.29$Hz

The theoretical and experimental results can be seen to be very close. Also the natural frequencies can be seen to be far separated.

In order to confirm that the beam behaves as a nonlinear system for large amplitude oscillations, it was excited by a harmonic force of frequency 10 Hz and relatively large amplitude as shown in Fig.4.6 (a). The response FFT shown in Fig.4.6 (b) shows a 3ω harmonic at 30 Hz., in addition to the harmonics at 20 Hz and 40 Hz., corresponding to the excitation frequency. Such test was carried out for various excitation frequencies, and the FFT of the response was characterised by the presence of 3ω harmonic, confirming the nonlinear behaviour of beam at large amplitude vibrations.

The sweep tests were then carried out for different acceleration and deceleration rates. Fig. 4.7(a) shows the excitation function, generated in the signal generator. The excitation frequency is swept from 0 Hz to 10 Hz. at a constant rate in 60 seconds. The response is shown in Fig. 4.7 (b). The peak vibrations can be seen to occur before the linear natural frequency (7.68 Hz). The excitation for deceleration from 10 Hz to 0 Hz in 60 seconds, is shown in Fig. 4.8 (a) and the corresponding response is given in Fig. 4.8 (b). The peak response while, decelerating can be observed to be at an instantaneous frequency lower,
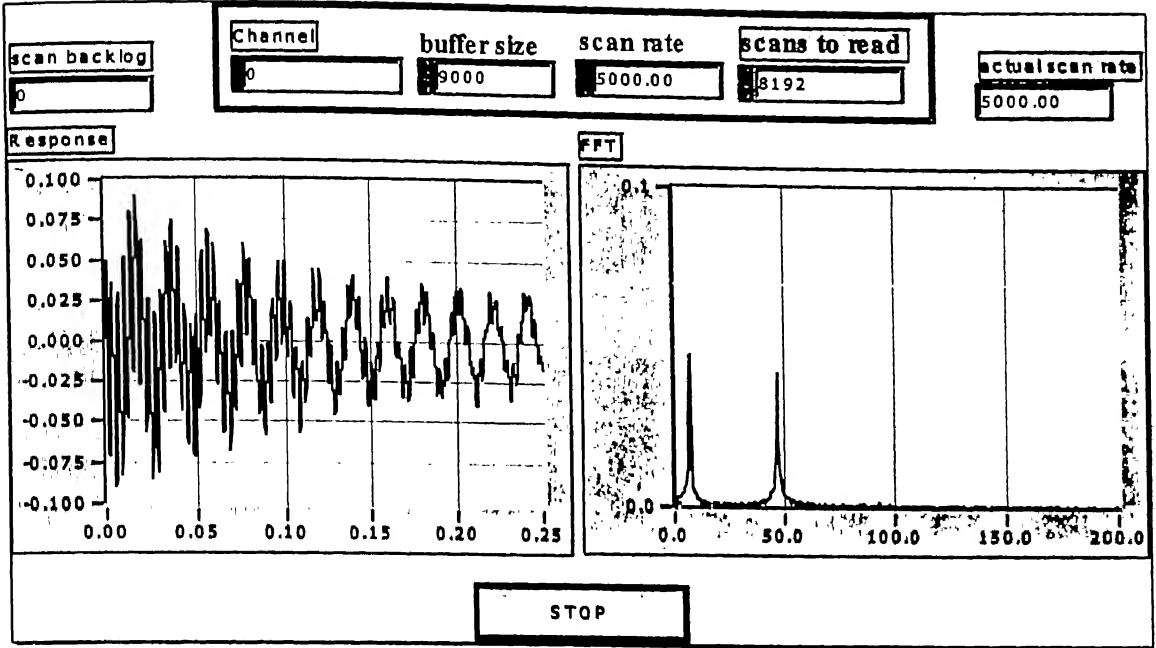
Fig. 4.5   Rap test results for identification of natural frequencies of beam.

than that while acceleration. Also, while deceleration the peak amplitude is higher than that during acceleration. This indicates a behaviour similar to a soft spring, with backbone curve bent to the left. The jump phenomenon can also be noticed from the figures. Figs. 4.7 (b) and 4.8 (b) also show the 1/3 subharmonics very clearly. The ½ subharmonic, if present seems to be very weak. This suggests that the system can be approximately modeled through an equation of the type

$$m\ddot{x} + c\dot{x} + k_1 x - k_3 x^3 = f_0 \sin \omega t$$

While $\sqrt{k_1/m} = \omega_1$, the first linear natural frequency of the system has already been identified during the Rap-Test as 7.68 Hz, no attempt has been made in the present study to identify the nonlinear stiffness value k_3.
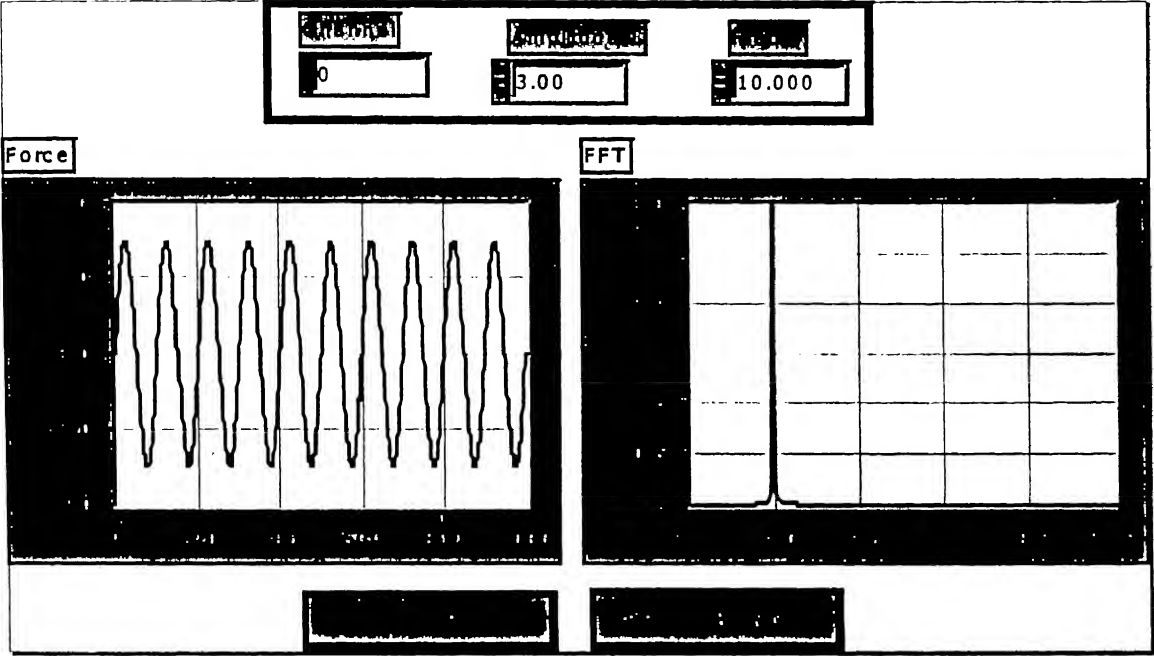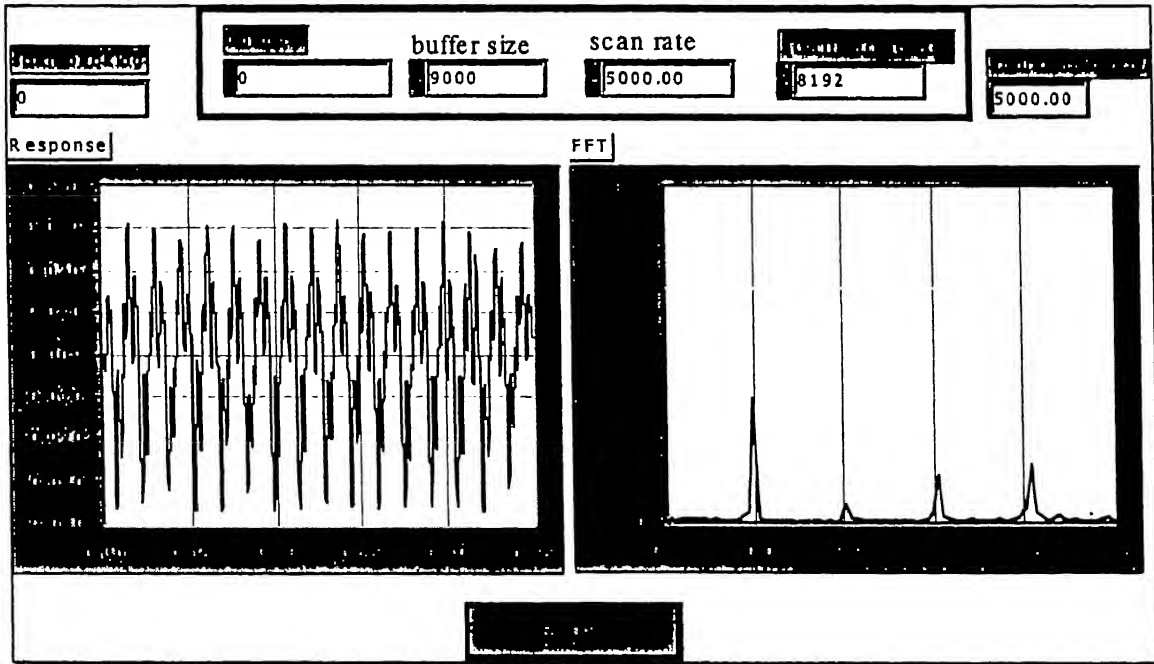
45

Fig. 4.6(a)   Constant excitation force

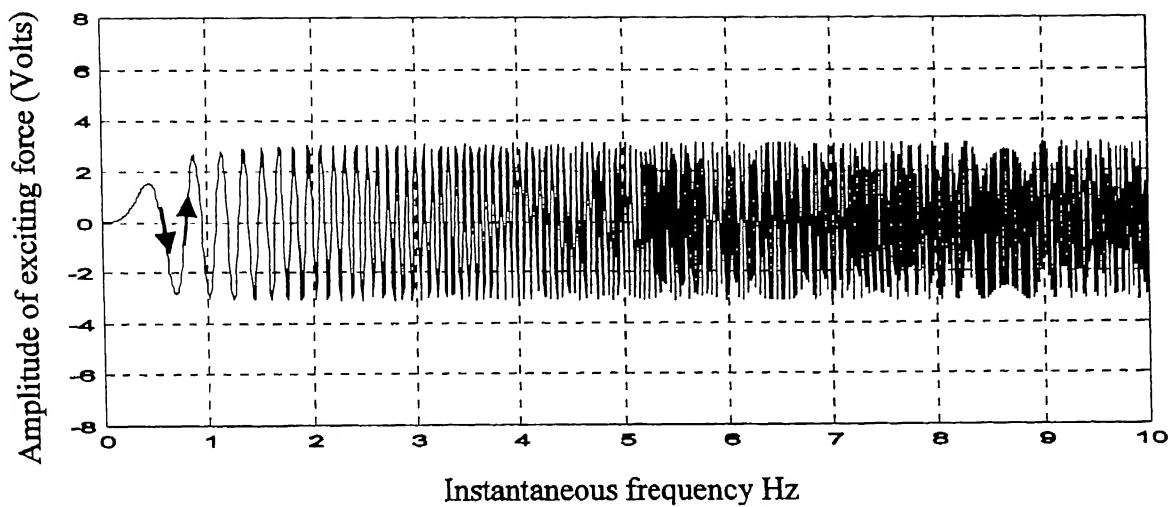**Fig. 4.6(b)   Response exhibiting nonlinearity of beam**

46

Fig. 4.7(a)   Excitation force with frequency swept from 0 to 10 Hz in 60 seconds.
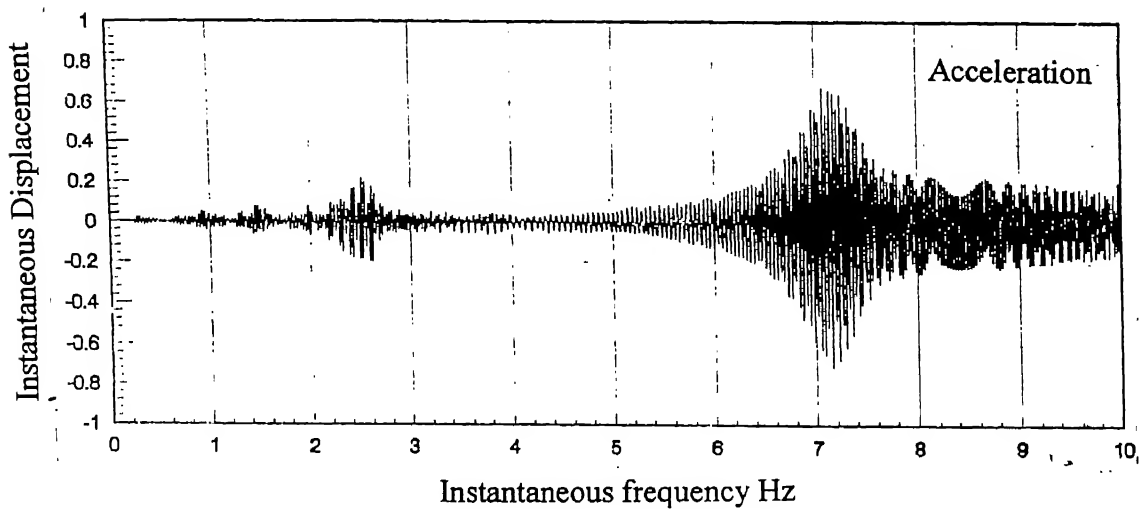

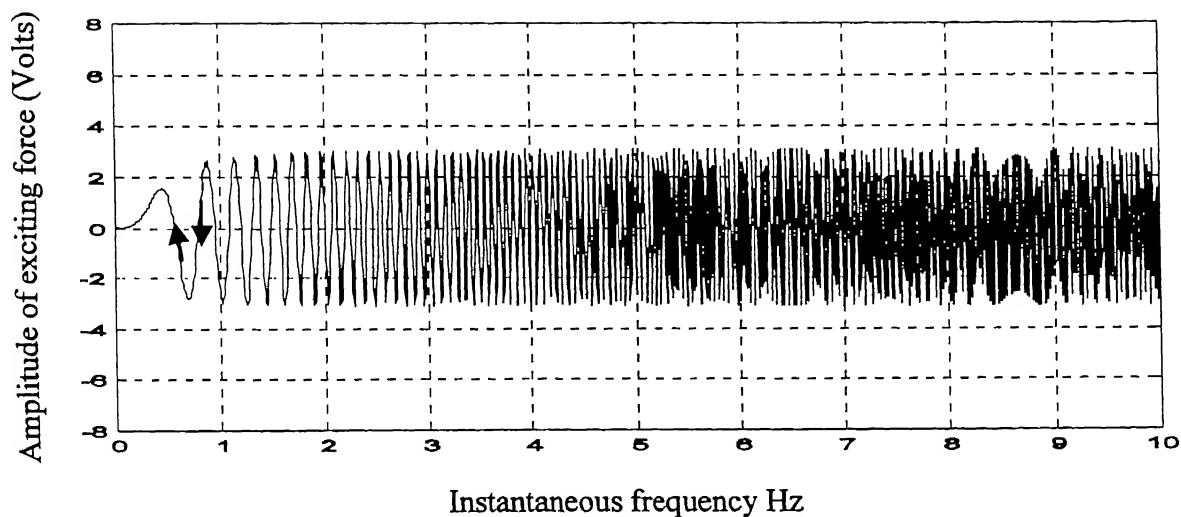**Fig. 4.7(b)   Non-stationary response of beam**

47

Fig. 4.8(a) Excitation force with frequency swept from 10 to 0 Hz in 60 seconds
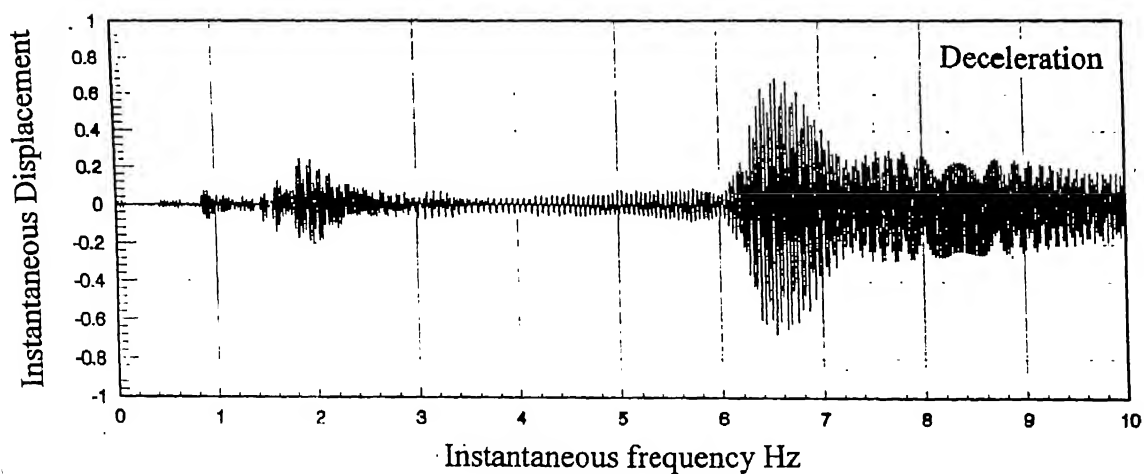

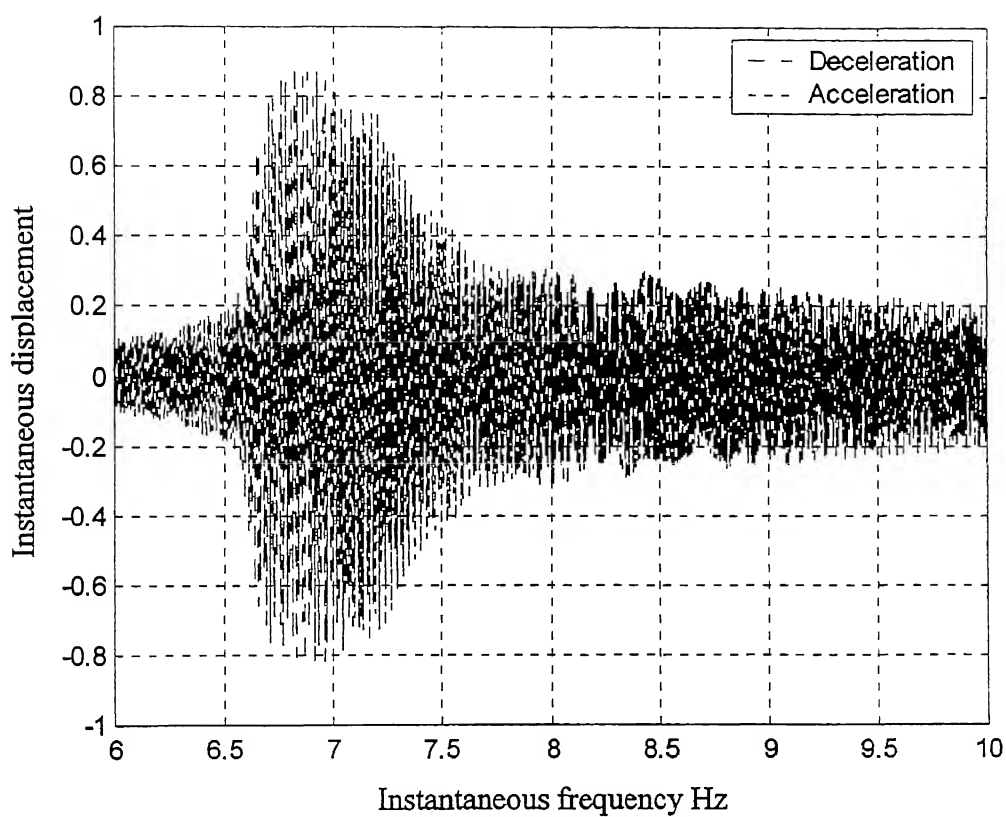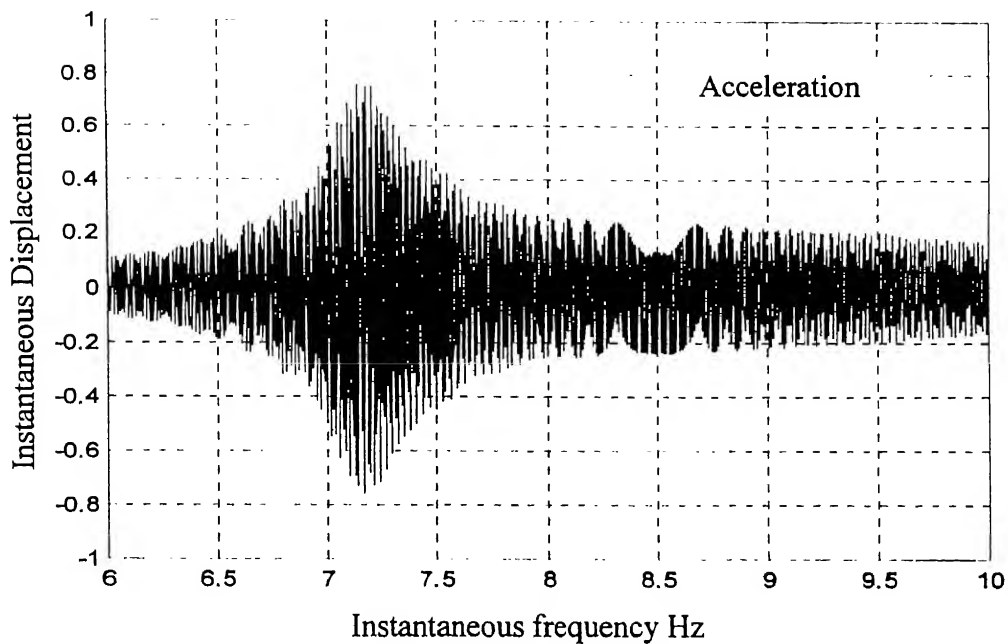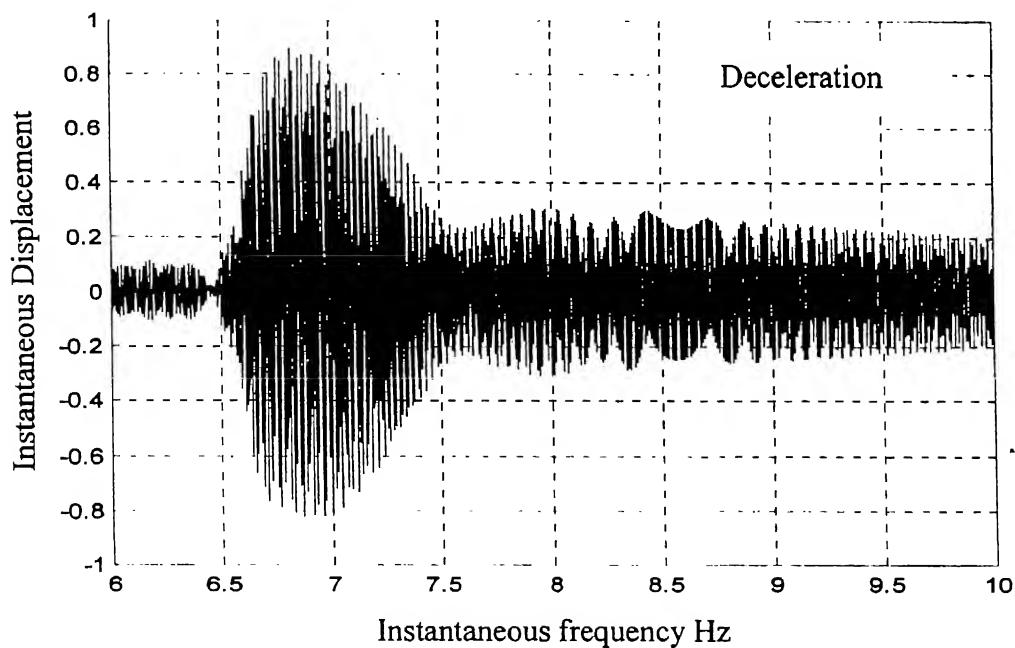**Fig. 4.8(b) Non-stationary response of beam**

48

Fig. 4.9   Superposition of Acceleration and Deceleration
(0 to 10 Hz in 80 seconds)

Superposisition of the response during acceleration and deceleration, as shown in Fig. 4.9, may help in providing information on the backbone curve. However, construction of such a curve from the experimental data, has also not been attempted during this study.

The response was obtained for different acceleration and deceleration rates. Fig. 4.10 (a), (b), show the response for acceleration and deceleration respectively, between 0 and 10 Hz in 100 seconds. Figs. 4.11 (a), (b) show the corresponding behaviour, when the transit time was reduced to 60 seconds while Figs. 4.12 (a), (b) show the response behaviour when transit time was further reduced to 40 seconds. It can be seen, through a comparative analysis of Figs. 4.8, 4.10 to 4.12, that with faster transit rates the peak response lowers in magnitude ih addition to showing greater shift away from the linear natural frequency value.

Fig. 4.10(a)   Non-stationary response during acceleration

(0 – 10 Hz in 100 seconds)

Fig. 4.10(b)   Non-stationary response during deceleration

(10 – 0 Hz in 100 seconds)

51
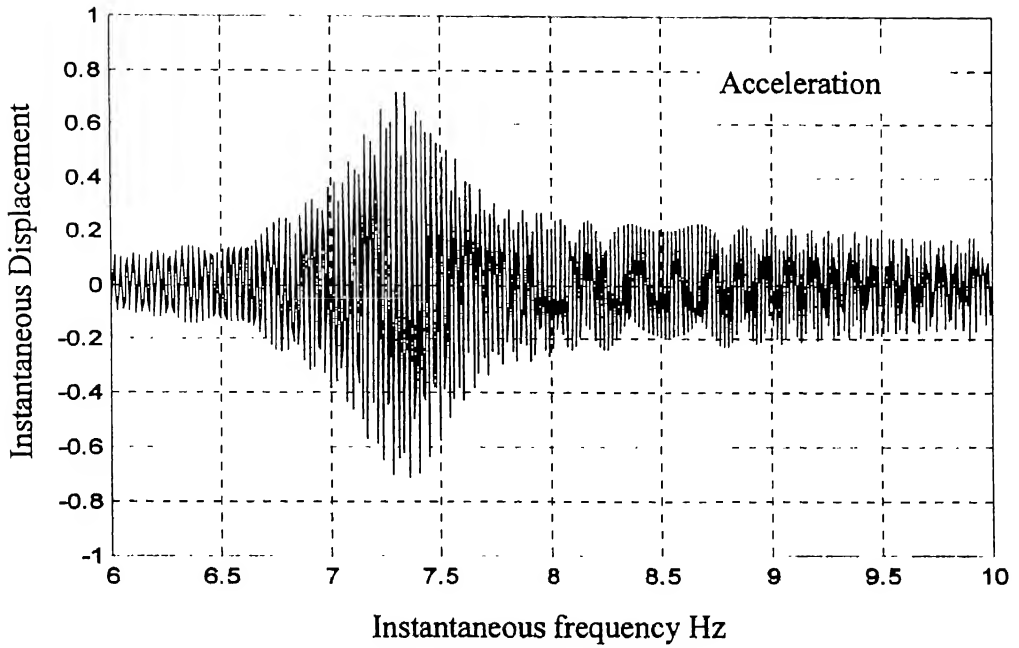
Fig. 4.11(a)   **Non-stationary response during acceleration**

(0 –10 Hz in 60 seconds)

Fig. 4.11(b)   **Non-stationary response during deceleration**
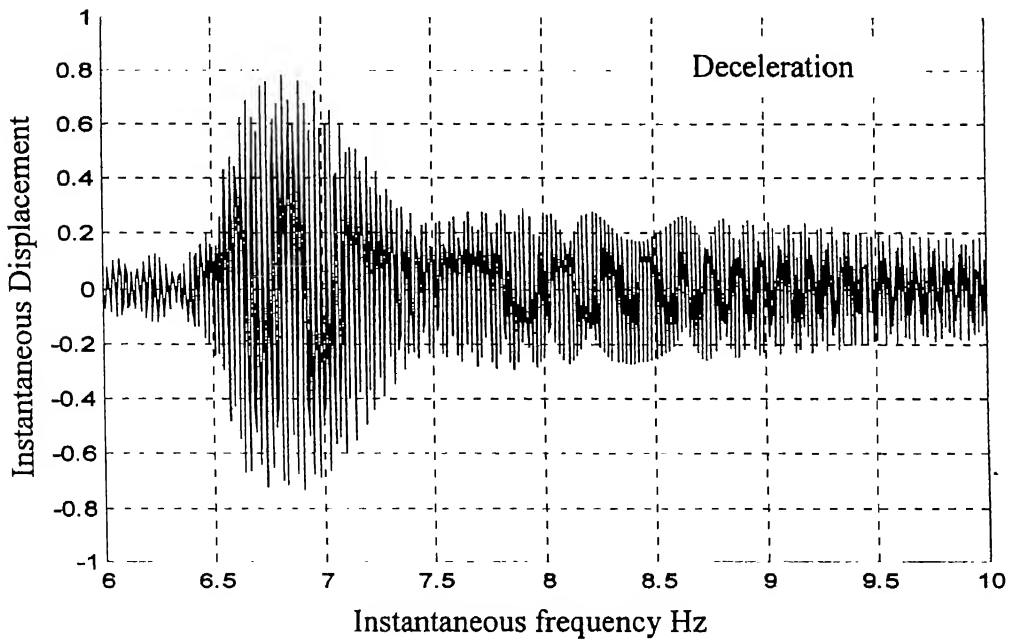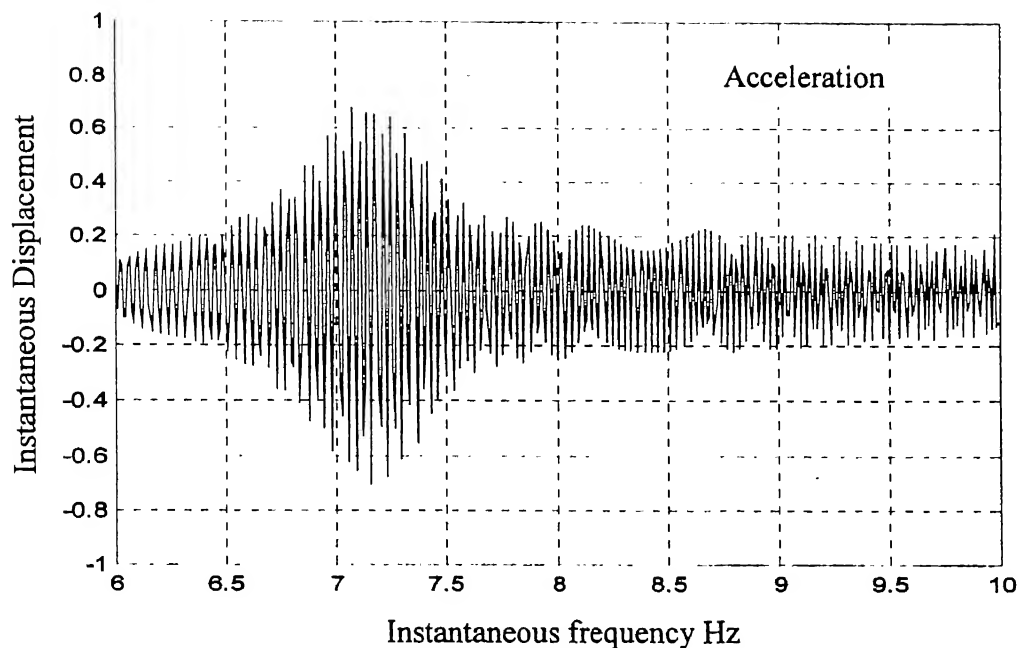
(10 – 0 Hz in 60 seconds)
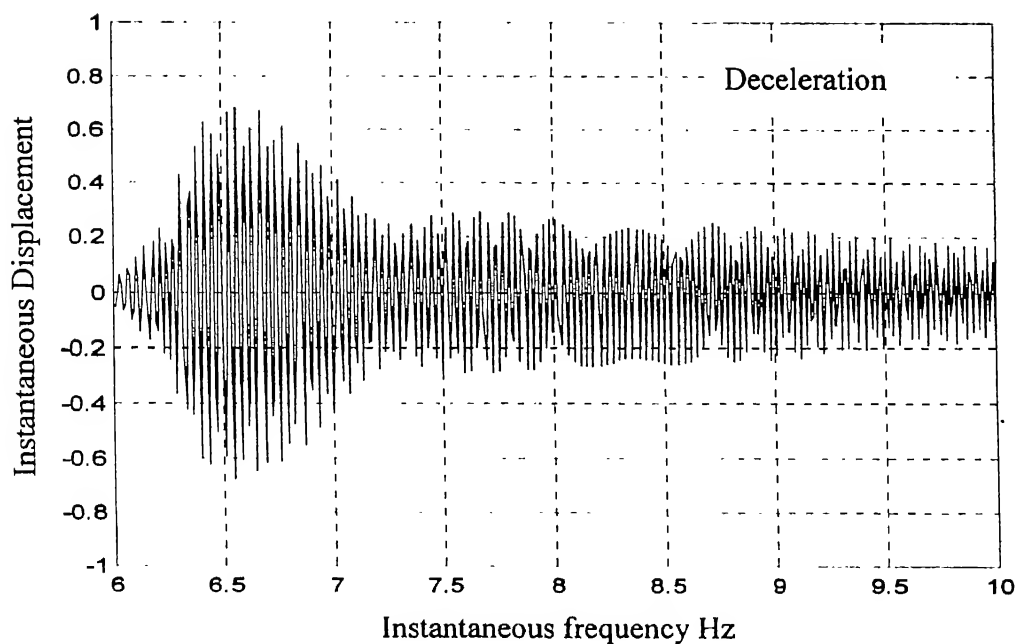
Fig. 4.12(a) Non-stationary response during acceleration

(0 –10 Hz in 40 seconds)

Fig. 4.12(b) Non-stationary response during deceleration

(10 –0 Hz in 40 seconds)

CHAPTER 5

CONCLUSIONS

The objective of the present study was to carry out numerical and experimental exercises to understand the behaviour of nonlinear systems subjected to harmonic excitation with constant variation in frequency. Some commonly encountered nonlinearities in mechanical systems were considered. An attempt was made to understand their behaviour by comparison with that of linear systems. The polynomial form of nonlinearity, specifically the cubic nonlinearity of a Duffing oscillator was further treated as benchmark for understanding peculiarities of other nonlinear systems. It was observed that the nonstationary behaviour of nonlinear systems is different from linear systems, in a variety of ways. A major feature of the nonlinear systems is that the response patterns, during acceleration and deceleration are not symmetric. The degree of asymmetry, is dependent on the type of nonlinearity, in addition to the rate of frequency change. For polynomial forms of nonlinearity, the assymmetry of these patterns is governed by the backbone curve. Lack of analytical models for other forms of nonlinearities, restricts their analysis to attempting piecewise polynomial approximations. These piecewise polynomial models help in justifying the presence of subharmonics in the response.

Experimental investigations, in addition to nonstationary vibration analysis, were also aimed at providing exercise in Virtual Instrumentation for Signal Generation as well as Data Acquisition. This task was successfully accomplished. The quality of the experimental results was observed to be good as distinct features of nonlinear behaviour during sweep tests could be clearly observed and rationalised.

Future numerical exercises can be carried out by incorporating damping nonlinearities also, in the models. The simplicity of the MATLAB Simulink models, make this task easy. Experimental investigations, in further studies can focus on systems like bearings, shafts etc. The Virtual Instruments developed can also be employed to investigate influence of cracks of various sizes and locations, on the nonlinear dynamics of beams.

REFERENCES

1. Bogoluibov.N.N., and Mitropol'skii Yu.A.,(1961) Asymptotic methods in the theory of nonlinear oscillations, Hindustan publishing co., Delhi.

2. Cunnigham.W.J., (1958) Introduction to nonlinear analysis, McGraw-Hill Inc, New York.

3. Evan-Iwanowski.R.M., (1976) Resonance oscillations in mechanical systems, Elsevier scientific publishing co., Amsterdam.

4. Gasch.R.,Markert.R and Pfutzner.H., (1979) Acceleration of unbalanced flexible rotors through the critical speeds, Journal of sound and vibrations, Vol. 63, No3, p 393-409.

5. Hayashi.C.,(1964) Nonlinear oscillations in mechanical systems, McGraw-Hill book co., New York.

6. Irretier.H.,(1984) Numerical analysis of transient responses in blade dynamics, Vibrations in Rotating machinery, Third Intl. conf., University of York., England, p255.

7. Ishida.Y., Yasuda.K. and Murakami.S.,(1997) Nonstationary oscillations of a rotating shaft with nonlinear spring characteristics during acceleration through a major critical speed (A discussion by the asymptotic method and the Complex-FFT method), Journal of Vibration and Acoustics, Vol. 119, p 31-36.

8. Krämer.E., (1993) Dynamics of rotors and foundations, Springer-Verlag, Heidelberg.

9. Lewis.F.M., (1932) Vibration during acceleration through a critical speed, ASME, Journal of applied mechanics, Vol. 54, p 253-257.

10. Mitropol'skii.Yu.A.,(1965) Problems of the asymptotic theory of Nonstationary vibrations, Daniel Davey and co. Inc., New York.

11. Nonami.K., Higashi.M. and Totani.T., (1988) A consideration of a method of passing through the critical speed of rotating shaft systems, JSME International journal, Vol 31, Series III, p 380-386.
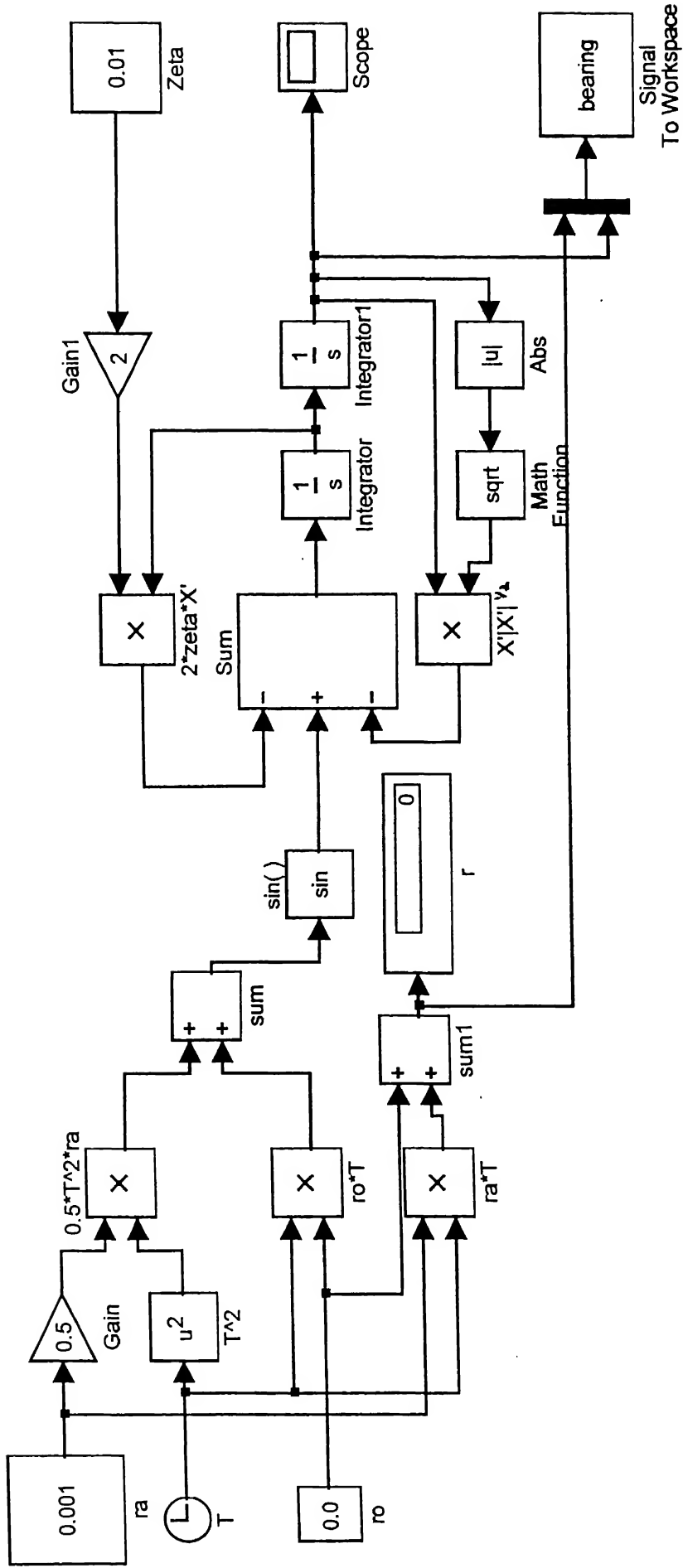
12. Schetzen.M., (1980) The Volterra and Wiener theories of nonlinear systems, John Wiley and sons, New York,.

13. Stoker.J.J., (1950) Nonlinear vibrations in mechanical and electrical systems, Interscience publishers Inc., New York.

14. Vyas.N.S., (1986) Vibratory stress analysis and fatigue life estimation of turbine blade, Ph.D. thesis dissertation, I.I.T. Delhi.
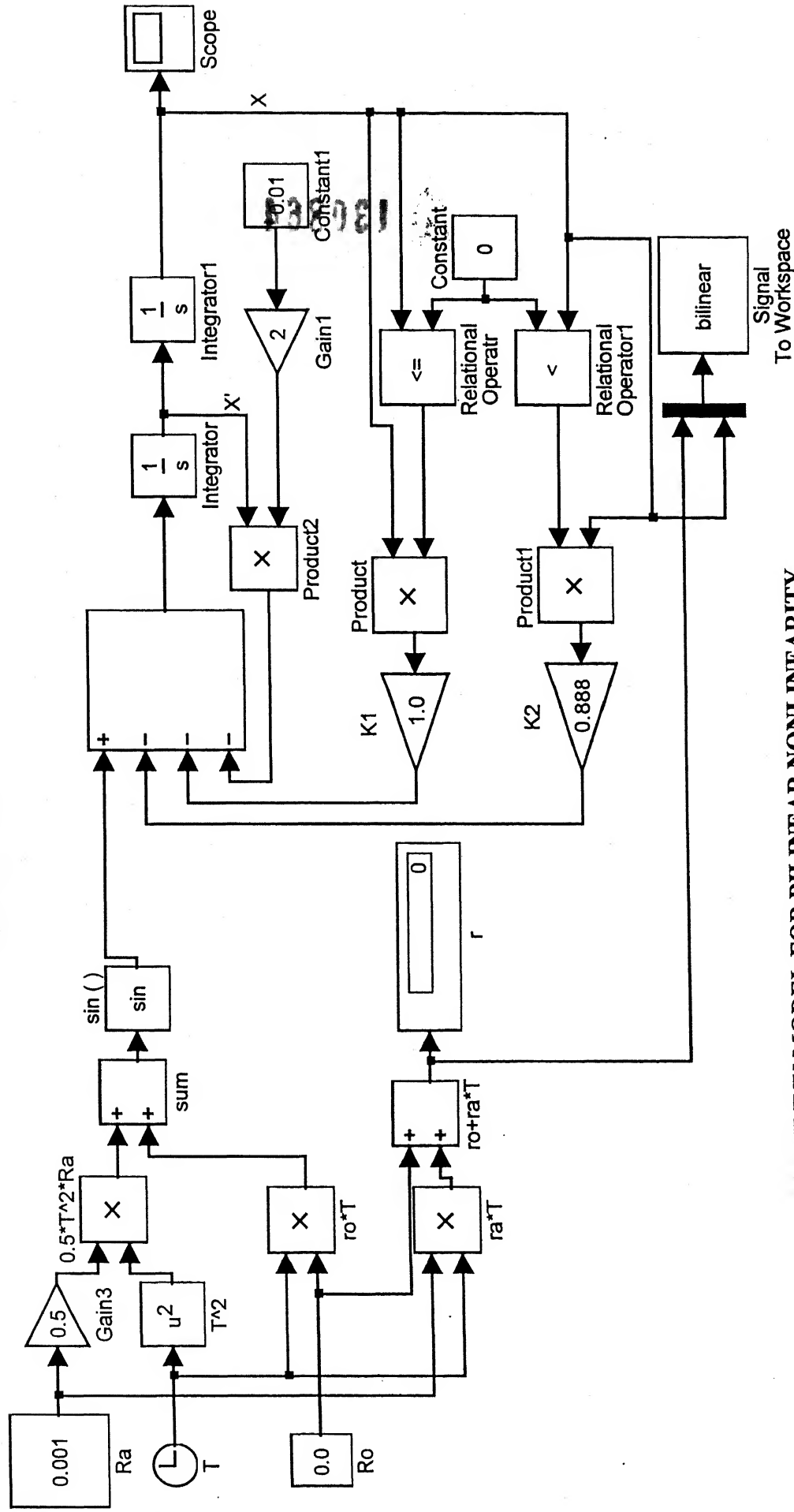
APPENDIX 1
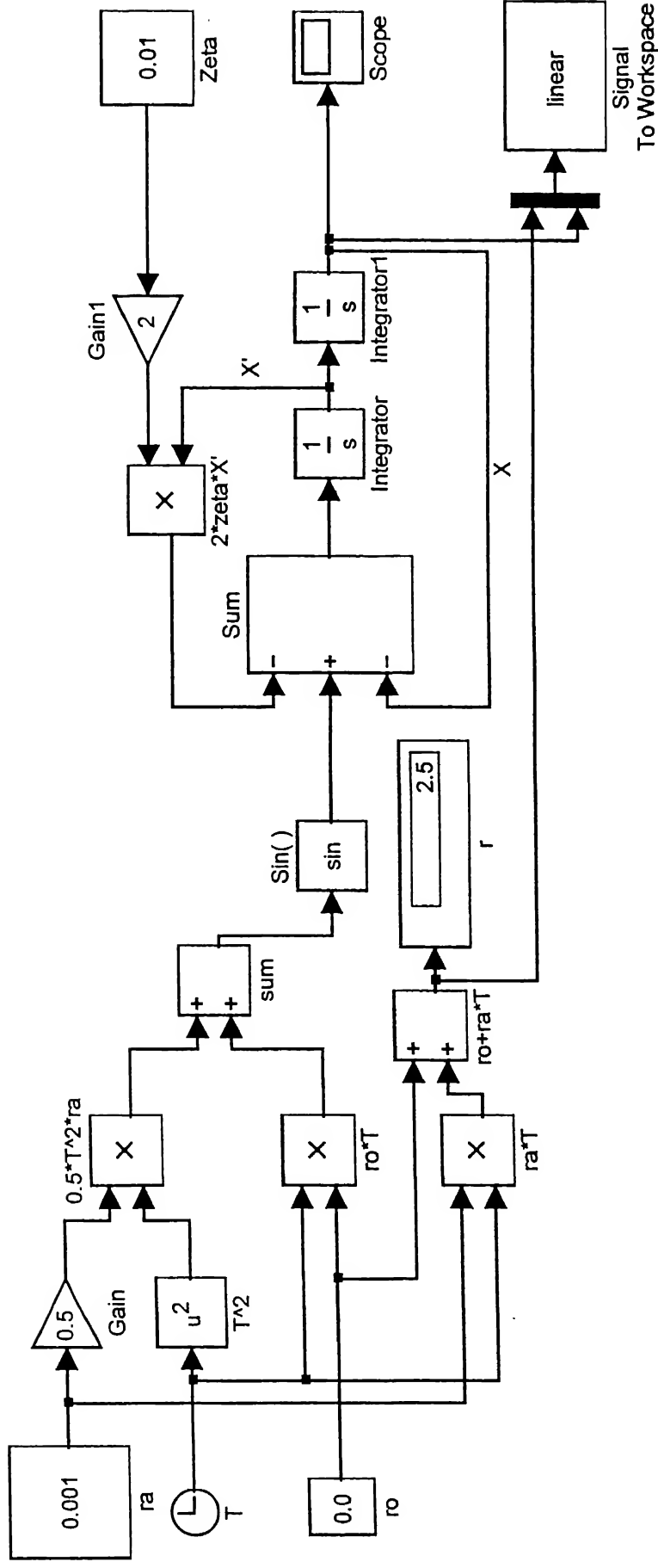
SIMULINK MODEL FOR LINEAR SYSTEM

APPENDIX 2

SIMULINK MODEL FOR CUBIC NONLINEARITY

APPENDIX 3

SIMULINK MODEL FOR SQUARE-CUBIC NONLINEARITY

APPENDIX 4

SIMULINK MODEL FOR SQUARE SYMMETRIC NONLINEARITY

APPENDIX 5

SIMULINK MODEL FOR BEARING NON LINEARITY

APPENDIX 6

SIMULINK MODEL FOR BILINEAR NONLINEARITY